

# Neutrino Mass Spectrum and Neutrinoless Double Beta Decay

H.V. Klapdor-Kleingrothaus, H. Päs

*Max-Planck-Institut für Kernphysik,*

*P.O. Box 103980, D-69029 Heidelberg, Germany*

A. Yu. Smirnov

*The Abdus Salam International Center of Theoretical Physics,*

*Strada Costiera 11, Trieste, Italy*

*Institute for Nuclear Research, RAS, Moscow, Russia*

## Abstract

The relations between the effective Majorana mass of the electron neutrino,  $m_{ee}$ , responsible for neutrinoless double beta decay, and the neutrino oscillation parameters are considered. We show that for any specific oscillation pattern  $m_{ee}$  can take any value (from zero to the existing upper bound) for normal mass hierarchy and it can have a minimum for inverse hierarchy. This means that oscillation experiments cannot fix in general  $m_{ee}$ . Mass ranges for  $m_{ee}$  can be predicted in terms of oscillation parameters with additional assumptions about the level of degeneracy and the type of hierarchy of the neutrino mass spectrum. These predictions for  $m_{ee}$  are systematically studied in the specific schemes of neutrino mass and flavor which explain the solar and atmospheric neutrino data. The contributions from individual mass eigenstates in terms of oscillation parameters have been quantified. We study the dependence of  $m_{ee}$  on the non-oscillation parameters: the overall scale of the neutrino mass and the relative mass phases. We analyze how forthcoming oscillation experiments will improve the predictions for  $m_{ee}$ . On the basis of these studies we evaluate the discovery potential of future  $0\nu\beta\beta$  decay searches. The role  $0\nu\beta\beta$  decay searches will play in the reconstruction of the neutrino mass spectrum is clarified. The key scales of  $m_{ee}$ , which will lead to the discrimination among various schemes are:  $m_{ee} \sim 0.1$  eV and  $m_{ee} \sim 0.005$  eV.

## 1 Introduction

The goal of the search for neutrinoless double beta decay ( $0\nu\beta\beta$  decay) is to establish the violation of (total) lepton number  $L$  and to measure the Majorana mass of the electron neutrino, thus identifying the nature of the neutrino [1, 2]. Both issues are related: Even if the main mechanism of  $0\nu\beta\beta$  decay may be induced by e.g. lepton number violating right-handed currents, R-parity violation in SUSY models, leptoquark-Higgs couplings (for an overview see e.g. [3]), the observation of  $0\nu\beta\beta$  decay implies always a non-vanishing effective neutrino Majorana mass ( $0\nu\beta\beta$ -mass) at loop level [4].

If  $0\nu\beta\beta$  decay is induced dominantly by the exchange of a light Majorana neutrino ( $m < 30$  MeV), the decay rate is proportional to the Majorana mass of the electron neutrino  $m_{ee}$  squared:

$$\Gamma \propto m_{ee}^2. \quad (1)$$

Thus, in absence of lepton mixing the observation of  $0\nu\beta\beta$  decay would provide an information about the absolute scale of the Majorana neutrino mass.

The situation is changed in presence of neutrino mixing when the electron neutrino is not a mass eigenstate but turns out to be a combination of several mass eigenstates,  $\nu_i$ , with mass eigenvalues  $m_i$ :

$$\nu_e = \sum_i U_{ei} \nu_i, \quad i = 1, 2, 3, \dots. \quad (2)$$

Here  $U_{ej}$  are the elements of the mixing matrix relating the flavor states to the mass eigenstates. In this general case the mass parameter ( $0\nu\beta\beta$ -mass) which enters the  $0\nu\beta\beta$  decay rate is not the physical mass of the neutrino but the combination  $m_{ee}$  of physical masses:

$$|m_{ee}| = \left| \sum_j |U_{ej}|^2 e^{i\phi_j} m_j \right|. \quad (3)$$

Apart from the absolute values of masses  $m_j$  and mixing matrix elements, the effective Majorana mass depends also on new parameters: phases  $\phi_j$  which originate from a possible complexity of the mass eigenvalues and from the mixing matrix elements. Thus searches for double beta decay are sensitive not only to masses but also to mixing matrix elements and phases  $\phi_j$ .

Notice that in the presence of mixing  $m_{ee}$  is still the  $ee$ -element of the neutrino mass matrix in the flavor basis<sup>1</sup>. In this sense it gives the scale of elements of the neutrino mass matrix. However, in general,  $m_{ee}$  does not determine the scale of the physical masses. If  $0\nu\beta\beta$  decay will be discovered and if it will be proven to proceed via the Majorana neutrino mass mechanism, then the  $m_{ee}$  extracted from the decay rate will give a lower bound on some physical masses. As it is easy to see from Eq. (3)), at least one physical mass,  $m_j$ , should be

$$m_j \geq \frac{m_{ee}}{3} \quad (4)$$

for the three-neutrino case.

Can  $m_{ee}$  be predicted? According to (3) the mass  $m_{ee}$  depends on absolute values of masses, mixings and phases  $\phi_j$ . Certain information about masses and mixing can be obtained from (i) oscillation searches, (ii) direct kinematical measurements and (iii) cosmology. Let us comment on these issues in order.

---

<sup>1</sup>In general the experimental value of  $m_{ee}$  depends on the process being considered. It coincides with the theoretical  $m_{ee}$  of eq. (3) if all masses  $m_i \ll Q$ , where  $Q$  is the energy release of a given process. This fact may become important for comparing heavy neutrino contributions in  $0\nu\beta\beta$  decay and inverse neutrinoless double beta decay at colliders, see *e.g.* [5].

1). The oscillation pattern is determined by mass squared differences, moduli of elements of the mixing matrix, and (for three neutrino mixing) only one complex phase which leads to CP violating effects in neutrino oscillations:

$$\Delta m_{ij}^2 \equiv |m_i|^2 - |m_j|^2, \quad |U_{ej}|^2, \quad \delta_{CP}. \quad (5)$$

(We indicated here only mixing elements which enter  $m_{ee}$ .) In what follows we will call (5) the *oscillation parameters*.

Neutrino oscillations and neutrinoless double beta decay, however, depend on different combinations of neutrino masses and mixings. In terms of the oscillation parameters the mass (3) can be rewritten as

$$|m_{ee}| = \left| \sum_j |U_{ej}|^2 e^{i\phi_j} \sqrt{\Delta m_{j1}^2 + m_1^2} \right|, \quad (6)$$

where we assumed for definiteness  $m_1$  to be the smallest mass. We also put  $\phi_1 = 0$  and consider the other  $\phi_j$  as the *relative phases*.

According to (6) the oscillation parameters do not allow one to determine uniquely  $m_{ee}$ . Apart from these parameters, the mass  $m_{ee}$  depends also on the absolute value of the first mass (absolute scale) and on the relative phases:

$$m_1, \quad \phi_j, \quad j = 2, 3, \dots \quad (7)$$

These parameters can not be determined from oscillation experiments and we will call them *non-oscillation parameters*.

The mass squared difference gives the absolute value of the mass only in the case of strong mass hierarchy:  $m_j \gg m_1$ , when  $|m_j| \approx \sqrt{\Delta m_{j1}^2}$ . However, even in this case the lightest mass (which can give a significant or even dominant contribution to  $m_{ee}$ ) is not determined.

The relative phases  $\phi_j$  which appear in  $m_{ee}$  (eq. (3)) differ from  $\delta_{CP}$  and can not be determined from oscillation experiments, since the oscillation pattern is determined by moduli  $|m_i|^2$ . On the other hand, the phase relevant for neutrino oscillations does not enter  $m_{ee}$  or can be absorbed in phases of masses.

2). Apart from neutrino oscillations, informations on neutrino masses and especially on the absolute scale of masses can be obtained from direct kinematical searches and cosmology.

There is still some chance that future kinematical studies of the tritium beta decay will measure the electron neutrino mass, and thus will allow us to fix the absolute scale of masses. Projects are under consideration which will have a sensitivity of about 1 eV and less (ref. [6]).

3). The expansion of the universe and its large scale structure are sensitive to neutrinos with masses larger than about 0.5 eV. The status of neutrinos as the hot dark matter (HDM) component of the universe is rather uncertain now: it seems that the present cosmological observations do not require a significant  $\Omega_\nu$  contribution and therefore a

large  $\mathcal{O}(1\text{eV})$  neutrino mass. However in some cases massive neutrinos may help to get a better fit of the data on density perturbations.

In order to predict  $m_{ee}$  one should not only determine the oscillation parameters but make additional assumptions which will fix the non-oscillation parameters. If the oscillation parameters are known, then, depending on these assumptions, one can predict  $m_{ee}$  completely or get certain bounds on  $m_{ee}$ .

What are these assumptions?

It was pointed out in [8] that predictions on  $m_{ee}$  significantly depend on two points:

- The level of degeneracy of the neutrino mass spectrum, which is related to the absolute scale of neutrino masses.
- The solution of the solar neutrino problem; this solution determines to a large extent the distribution of the electron neutrino flavor in the mass eigenstates, that is,  $|U_{ej}|^2$ .

The assumptions about the level of degeneracy allow one to fix the absolute scale of the neutrino mass. In fact, at present even the oscillation parameters are essentially unknown, so that further assumptions are needed. Evidences of neutrino oscillations (atmospheric, solar neutrino problems, LSND result) allow us in principle to determine the oscillation parameters up to a certain ambiguity related, in particular, to the existence of several possible solutions of the solar neutrino problem.

A number of studies of the  $0\nu\beta\beta$ -mass have been performed, using various assumptions about the hierarchy/degeneracy of the spectrum which remove the ambiguity in interpretations of existing oscillation data. In fact, these assumptions allow one to construct the neutrino mass and mixing spectrum, and some studies have been performed for specific neutrino spectra. Most of the spectra considered so far explain the atmospheric neutrino problem and the solar neutrino problem assuming one of the suggested solutions. Some results have also been obtained for schemes with 4 neutrinos which also explain the LSND result. Let us summarize the main directions of these studies.

(1) Three-neutrino schemes with normal mass hierarchy which explain the solar and atmospheric neutrino data have been studied in [8, 9, 10, 11, 12, 13]. Various solutions of the  $\nu_\odot$ -problem were assumed. These schemes give the most stringent constraints on  $0\nu\beta\beta$ -mass in terms of oscillation parameters.

(2) The  $0\nu\beta\beta$ -mass in three-neutrino schemes with inverse mass hierarchy has been considered in [14, 12, 13]. These schemes favor  $m_{ee}$  to be close to the present experimental bound.

(3) Three-neutrino schemes with *partial* degeneracy of the spectrum and various solutions of the  $\nu_\odot$ -problem were discussed in [8, 13]. In these schemes  $m_{ee}$  can also be close to the present experimental bound.

(4) Large attention was devoted to the three-neutrino schemes with complete degeneracy [8, 15, 16, 17, 18, 19, 20, 21, 22, 23, 13] since they can explain solar and atmospheric neutrino data and also give a significant amount of the HDM in the universe. In these schemes the predictions of  $m_{ee}$  depend mainly on the absolute mass scale and on the mixing angle relevant for the solar neutrinos.

Some intermediate situations between hierarchical and degenerate spectra have been discussed in [19, 13].

5. The  $0\nu\beta\beta$ -mass in scenarios with 4 neutrinos which can accommodate also the LSND result have been analyzed in Ref. [14, 10, 11].

Some general bounds on the  $0\nu\beta\beta$ -mass under various assumptions have been discussed in [24, 25, 26, 19, 27, 28].

In a number of papers an inverse problem has been solved: using relations between the  $0\nu\beta\beta$ -mass and oscillation parameters which appear in certain schemes restrictions on oscillation parameters have been found from existing bounds on  $m_{ee}$ . In particular the  $3\nu$ -schemes with mass degeneracy [15] and mass hierarchy [12] have been discussed.

An important ingredient for the prediction of  $m_{ee}$  are the phases (see eq. 7). Unfortunately, there is no theory or compelling assumptions which allow to determine these phases.

In this paper we will analyze the discovery potential of future  $0\nu\beta\beta$  decay searches in view of existing and forthcoming oscillation experiments. We will clarify the role  $0\nu\beta\beta$  decay searches will play in the identification of the neutrino mass spectrum.

For this we first (sect. 2) consider the general relations between the effective Majorana mass of the electron neutrino and the oscillation parameters. We will study the dependence of  $m_{ee}$  on the non-oscillation parameters. The crucial assumptions which lead to predictions for  $m_{ee}$  are identified.

In sects. 3 - 7 we present a systematic and updated study of predictions for  $m_{ee}$  for possible neutrino mass spectra. In contrast with most previous studies using oscillation data we quantify the contributions from *individual* mass eigenstates and we keep explicitly the dependence on unknown relative mass phases. The dependence of predictions on non-oscillation parameters – the absolute mass value and the phases  $\phi_i$  is studied in detail. We consider  $3\nu$ -schemes with mass hierarchy (section 3), partial degeneracy (section 4), inverse hierarchy (section 5), total degeneracy (section 6) and schemes with sterile neutrinos (section 7). We analyse how forthcoming and planned oscillation experiments will sharpen the predictions for  $m_{ee}$ . In sect. 8, comparing predictions of  $m_{ee}$  from different schemes we clarify the role future searches for  $0\nu\beta\beta$  decay can play in the identification of the neutrino mass spectrum.

## 2 Neutrino oscillations and neutrinoless double beta decay

As has been pointed out in the introduction, the prediction of  $m_{ee}$  depends on oscillation ( $|U_{ei}|$ ,  $\Delta m^2$ ) and non-oscillation ( $m_1$  and  $\phi_j$ ) parameters. In this section we will consider general relations between  $m_{ee}$  and the oscillation parameters. We analyse the dependence of these relations on non-oscillation parameters. We quantify ambiguities which exist in predictions of  $m_{ee}$ . Our results will be presented in a way which will be convenient for implementations of future oscillation results.

## 2.1 Effective Majorana mass and oscillation parameters

The oscillation pattern is determined by the effective Hamiltonian (in the flavor basis):

$$H = \frac{1}{2E} MM^\dagger + V , \quad (8)$$

where  $E$  is the neutrino energy,  $M$  is the mass matrix and  $V$  is the (diagonal) matrix of effective potentials which describe the interaction of neutrinos in a medium.

The oscillation pattern is not changed if we add to  $H$  a term proportional to the unity matrix:

$$MM^\dagger \rightarrow MM^\dagger \pm m_0^2 I . \quad (9)$$

Indeed, the additional term does not change the mixing, it leads just to a shift of the mass eigenstates squared by the same value without affecting  $\Delta m_{ij}^2$ :

$$m_i^2 \rightarrow m_i^2 \pm m_0^2 . \quad (10)$$

(we consider  $m_i^2 - m_0^2 \geq 0$  for all  $i$  to keep the Hermiticity of the Hamiltonian). The additional term changes, however, the  $0\nu\beta\beta$ -mass. Thus, for a given oscillation pattern there is a freedom in  $m_{ee}$ , associated with  $m_0^2$ .

Let us study how arbitrary  $m_{ee}$  can be for a given oscillation pattern. According to (9,10) for the three-neutrino case we get

$$m_{ee} = |m_{ee}^{(1)}| + e^{i\phi_2} |m_{ee}^{(2)}| + e^{i\phi_3} |m_{ee}^{(3)}| , \quad (11)$$

where  $m_{ee}^{(i)} \equiv |m_{ee}^{(i)}| \exp(i\phi_i)$  ( $i = 1, 2, 3$ ) are the contributions to  $m_{ee}$  from individual mass eigenstates which can be written in terms of oscillation parameters as:

$$|m_{ee}^{(1)}| = |U_{e1}|^2 m_1, \quad (12)$$

$$|m_{ee}^{(2)}| = |U_{e2}|^2 \sqrt{\Delta m_{21}^2 + m_1^2}, \quad (13)$$

$$|m_{ee}^{(3)}| = |U_{e3}|^2 \sqrt{\Delta m_{31}^2 + m_1^2}. \quad (14)$$

and  $\phi_i$  are the relative phases of the contributions from masses  $m_i$  and  $m_j$  (the mass  $m_0^2$  has been absorbed in definition of  $m_1^2$ ). The contributions  $m_{ee}^{(i)}$  can be shown as vectors in the complex plane (fig. 1).

Without loss of generality we assume  $m_3 > m_2 > m_1 \geq 0$ , so that  $m_1$  is the lightest state. Then *normal* mass hierarchy corresponds to the case when the electron flavor prevails in the lightest state:  $|U_{e1}|^2 > |U_{e2}|^2, |U_{e3}|^2$ . We will refer to *inverse* hierarchy as to the case when  $|U_{e1}|^2 < |U_{e2}|^2$  or/and  $|U_{e3}|^2$ , *i.e.* when the admixture of the electron neutrino flavor in the lightest state is not the largest one.

Let us consider the dependence of  $m_{ee}$  on *non-oscillation parameters*  $m_{ee} = m_{ee}(m_1, \phi_j)$ . It is obvious that due to the freedom in the choice of  $m_1$  there is no upper bound for  $m_{ee}$ . However, in some special cases lower bounds on  $m_{ee}$  exist.

Let us start with the two neutrino case which would correspond to zero (or negligibly small)  $\nu_e$  admixture in one of mass eigenstates, *e.g.*  $|U_{e3}|$ . We consider first the case of

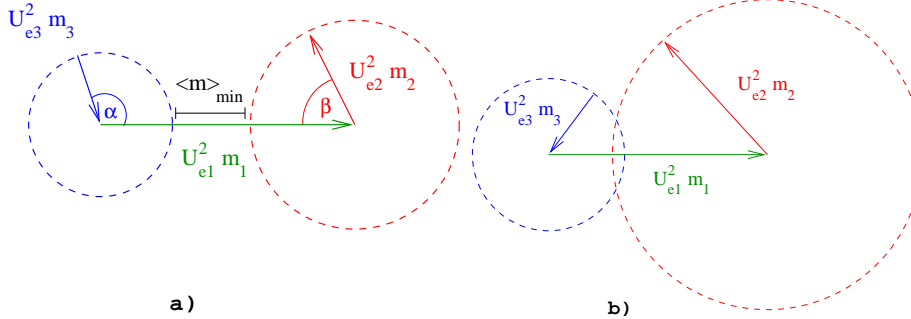


Figure 1: The effective Majorana mass  $m_{ee}$  in the complex plane. Vectors show contributions to  $m_{ee}$  from individual eigenstates. The total  $m_{ee}$  appears as the sum of the three vectors. Allowed values of  $m_{ee}$  correspond to modulies of vectors which connect two points on the circles. Here  $\alpha = \phi_3 - \pi$ ,  $\beta = \pi - \phi_2$ . a).  $|m_{ee}^{(1)}| > |m_{ee}^{(2)}| + |m_{ee}^{(3)}|$ : the vectors  $\vec{m}_{ee}^{(i)}$  can not form a triangle and no complete cancellation occurs. b)  $|m_{ee}^{(1)}| \leq |m_{ee}^{(2)}| + |m_{ee}^{(3)}|$ : in this case complete cancellation occurs in the intersection points of the circles, so that  $m_{ee} = 0$ .

normal hierarchy  $U_{e1}^2 > U_{e2}^2$ . For  $m_1 = 0$  the effective mass  $m_{ee}$  is uniquely fixed in terms of oscillation parameters:

$$m_{ee}^0 = |U_{e2}|^2 \sqrt{\Delta m_{21}^2} \equiv \sin^2 \theta \sqrt{\Delta m_{21}^2}, \quad (15)$$

where  $\sin \theta \equiv U_{e2}$ . For non-zero  $m_1$ , the maximal and minimal values of  $m_{ee}$  correspond to  $\phi_2 = 0$  and  $\phi_2 = \pi$ .

The upper bound ( $\phi_2 = 0$ ) on  $m_{ee}$  increases with  $m_1$  monotonously from  $m_{ee}^0$  at  $m_1 = 0$  and approaches the asymptotic dependence  $m_{ee} = m_1$  for large  $m_1$  (see fig. 2 a). The lower limit ( $\phi_2 = \pi$ ) decreases monotonously with increase of  $m_1$  starting by  $m_{ee}^0$ . It reaches zero at

$$m_1 = \frac{\sin^2 \theta}{\sqrt{|\cos 2\theta|}} \sqrt{\Delta m_{21}^2}, \quad (16)$$

and approaches the asymptotic dependence  $m_{ee} = |\cos 2\theta| m_1$  at large  $m_1$  (see fig. 2 a). Thus, for arbitrary values of oscillation parameters, no bound on  $|m_{ee}|$  exists.

(2) In the case of inverse hierarchy,  $|U_{e2}| > |U_{e1}|$ , the function  $m_{ee}(m_1)$  has a minimum which differs from zero,

$$m_{ee}^{\min} = \sqrt{|\cos 2\theta| \Delta m_{21}^2} \quad (17)$$

at

$$m_1 = \frac{\cos^2 \theta}{\sqrt{|\cos 2\theta|}} \sqrt{\Delta m_{21}^2}. \quad (18)$$

At large  $m_1$  it has the asymptotics  $m_{ee} = |\cos 2\theta| m_1$ . (fig. 2 b). As we will see, the existence of a minimal value of  $|m_{ee}|$  can play an important role in the discrimination of various scenarios.

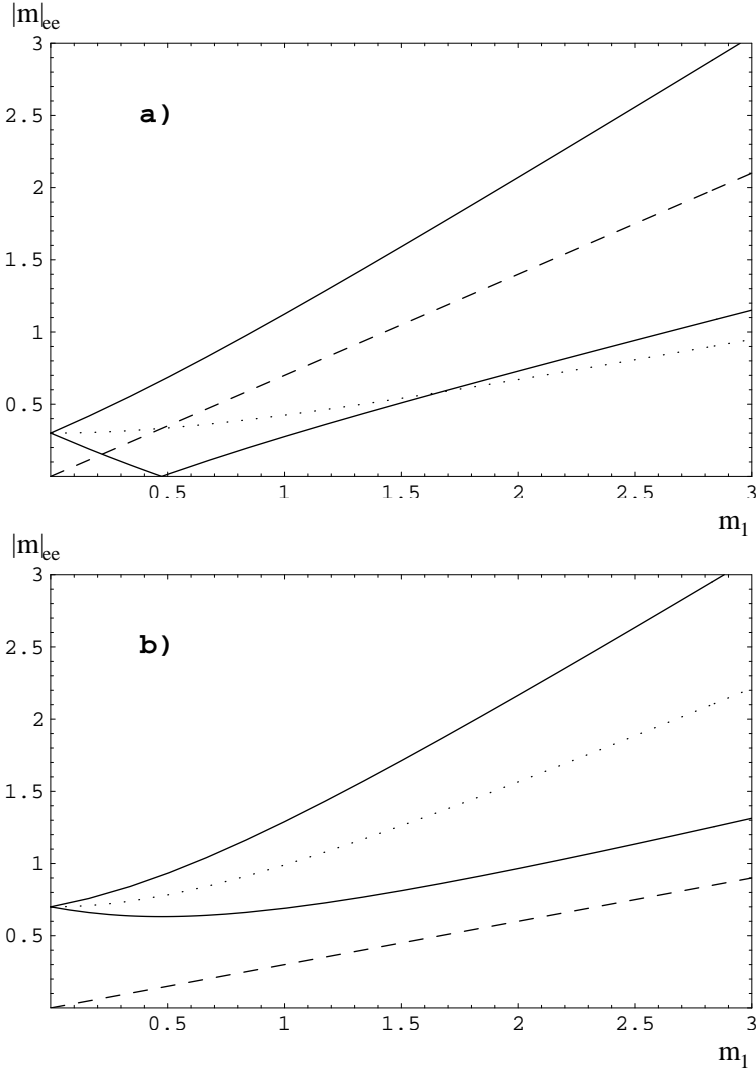


Figure 2: Qualitative dependence of the effective Majorana mass  $m_{ee}$  on  $m_1$  in the two neutrino mixing case. a) corresponds to the case of normal mass hierarchy, b) to the case of inverse hierarchy. Shown are the contributions  $m_{ee}^{(1)}$  (dashed) and  $m_{ee}^{(2)}$  (dotted). The solid lines give  $m_{ee}^{max}$  and  $m_{ee}^{min}$ , which correspond to  $\phi_{21} = 0$  and  $\phi_{21} = \pi$ , respectively. While in the case of normal hierarchy a complete cancellation is possible, so that  $m_{ee} = 0$ , for inverse hierarchy a minimal value  $|m_{ee}^{min}| > 0$  exists.

Let us consider now the three-neutrino case. The mass  $m_{ee}$  is given by the sum of three vectors  $\vec{m}_{ee}^{(1)}$ ,  $\vec{m}_{ee}^{(2)}$  and  $\vec{m}_{ee}^{(3)}$  in the complex plane (see fig. 1), so that a complete cancellation corresponds to a closed triangle. The sufficient condition for having a minimal value of  $|m_{ee}|$  which differs from zero for arbitrary non-oscillation parameters is

$$|m_{ee}^{(i)}| > \sum_{j \neq i} |m_{ee}^{(j)}|. \quad (19)$$

That is, one of contributions  $m_{ee}^{(i)}$  should be larger than the sum of the moduli of the two

others.

Let us prove that this condition can not be satisfied for the *normal* hierarchy case. Indeed, in eq. (19)  $i$  can not be 1. For  $m_1 = 0$  we have  $m_{ee}^{(1)} = 0$ , at the same time the right-handed side of eq. (19) is larger than zero as long as  $U_{e1}^2 \neq 1$ , (*i.e.* any non-zero mixing of  $\nu_e$  exists). The condition (19) can not be satisfied for  $i \neq 1$  either. In this case for a large enough  $m_1$ , so that  $m_1 \simeq m_2 \simeq m_3$ , we get  $m_{ee}^{(i)} < m_{ee}^{(1)}$  since  $U_{e1} > U_{ei}$ . This proof holds also for schemes with more than three neutrinos. Thus, one can conclude that neither an upper nor a lower bound on  $|m_{ee}|$  exists for any oscillation pattern and normal mass hierarchy. Any value  $|m_{ee}| \geq 0$  can be obtained by varying the non-oscillation parameters  $m_1$  and  $\phi_{ij}$ .

For inverse mass hierarchy we find that condition eq. (19) can be fulfilled for  $i = 3$ . Since now both  $m_3 > m_2, m_1$  and  $U_{e3} > U_{e2}, U_{e1}$  one can get

$$m_3|U_{e3}|^2 > m_2|U_{e2}|^2 + m_1|U_{e1}|^2 \quad (20)$$

for any set of values of non-oscillation parameters provided that the mixing of the heaviest state fulfills

$$|U_{e3}|^2 > 0.5. \quad (21)$$

Indeed, for large enough  $m_1$ , such that  $m_1 \simeq m_2 \simeq m_3$ , the condition (20) reduces to  $|U_{e3}|^2 > |U_{e2}|^2 + |U_{e1}|^2 \equiv 1 - |U_{e3}|^2$ , and the latter is satisfied for (21). For smaller values of  $m_1$  the relative difference of masses  $m_3 > m_2, m_1$  increases and the inequality of contributions in eq. (20) becomes even stronger. Thus, the inequality (21) is the sufficient condition for all values of  $m_1$ . This statement is true also for any number of neutrinos. It is also independent of the relative size of  $U_{e2}$  and  $U_{e1}$ .

Summarizing we conclude that

- No upper bound on  $|m_{ee}|$  can be derived from oscillation experiments.
- A lower bound exists only for scenarios with inverse mass hierarchy when the heaviest state ( $\nu_3$ ) mixes strongly with the electron neutrino:  $|U_{e3}|^2 > 0.5$ .  
For normal mass hierarchy certain values of the non-oscillation parameters  $m_1, \phi_j$  exist for which  $m_{ee} = 0$ .

The cases of normal and inverse mass hierarchy (they differ by signs of  $\Delta m^2$  once the flavor of the states is fixed) can not be distinguished in vacuum oscillations. However, it is possible to identify the type of the hierarchy in studies of neutrino oscillations in matter, since matter effects depend on the relative signs of the potential  $V$  and  $\Delta m_{ij}^2$ . This will be possible in future atmospheric neutrino experiments, long base-line experiments and also studies of properties of the neutrino bursts from supernova [37].

## 2.2 Effective Majorana mass and the degeneracy of the spectrum

As follows from fig. 2, predictions for  $m_{ee}$  can be further restricted under assumptions about the absolute scale of neutrino masses  $m_1$ . With increase of  $m_1$  the level of degeneracy of the neutrino spectrum increases and we can distinguish three extreme cases:

- $m_1^2 \ll \Delta m_{21}^2 \ll \Delta m_{31}^2$ , in this case the spectrum has a strong *mass hierarchy*.
- $\Delta m_{21}^2 \ll m_1^2 \ll \Delta m_{31}^2$ , this is the case of *partial* degeneracy;
- Inequality  $\Delta m_{21}^2 \ll \Delta m_{31}^2 \ll m_1^2$  corresponds to *strong* degeneracy.

There are also two transition regions when  $m_1^2 \sim \Delta m_{21}^2$  and  $m_1^2 \sim \Delta m_{31}^2$ . In what follows we will consider all these cases in order.

## 2.3 Effective Majorana mass and present oscillation data

Present oscillation data do not determine precisely all oscillation parameters. The only conclusion that can be drawn with high confidence level is that the muon neutrino has large (maximal) mixing with some non-electron neutrino state. The channel  $\nu_\mu \leftrightarrow \nu_\tau$  is the preferable one, and it is the only possibility, if no sterile neutrino exists. Thus, in  $3\nu$  schemes the atmospheric neutrino data are described by  $\nu_\mu \leftrightarrow \nu_\tau$  oscillations as dominant mode with

$$\Delta m_{atm}^2 = (2 \div 6) \cdot 10^{-3} \text{eV}^2, \quad \sin^2 2\theta_{atm} = 0.84 - 1, \quad (22)$$

and the best fit point

$$\Delta m_{atm}^2 = 3.5 \cdot 10^{-3} \text{eV}^2, \quad \sin^2 2\theta_{atm} = 1.0, \quad (23)$$

[29], see also [30]. A small contribution of the  $\nu_\mu \leftrightarrow \nu_e$  mode is possible and probably required in view of an excess in the  $e$ -like events in the Super-K experiment.

As it was realized some time ago [8], predictions for  $m_{ee}$  depend crucially on the solution of the solar neutrino problem. The solution of the solar neutrino problem determines the distribution of the  $\nu_e$ -flavor in the mass eigenstates, and this affects considerably expectations for the  $0\nu\beta\beta$ -mass. Up to now the unique solution is not yet identified and there are several possibilities [31], see also [32]:

1. Small mixing angle MSW solution with

$$\Delta m_\odot^2 = (0.4 \div 1) \cdot 10^{-5} \text{eV}^2, \quad \sin^2 2\theta_\odot = (0.2 \div 1.2) \cdot 10^{-2} \quad (24)$$

2. Large mixing angle MSW solution with

$$\Delta m_\odot^2 = (0.1 \div 1.5) \cdot 10^{-4} \text{eV}^2, \quad \sin^2 2\theta_\odot = (0.53 \div 1) \quad (25)$$

3. Low mass MSW (LOW) solution with

$$\Delta m_\odot^2 = (0.3 \div 2.5) \cdot 10^{-7} \text{eV}^2, \quad \sin^2 2\theta_\odot = (0.8 \div 1) \quad (26)$$

4. Several regions of vacuum oscillation (VO) solutions exist with

$$\Delta m_{\odot}^2 < 10^{-9} \text{ eV}^2, \quad \sin^2 2\theta_{\odot} > 0.7. \quad (27)$$

There is a good chance that before the new generation of double beta decay experiments starts operation studies of the solar neutrino fluxes by existing and forthcoming experiments will allow us to identify the solution of the solar neutrino problem. The key measurements include the day-night effect, the zenith angle dependence of the signal during the night, seasonal variations, energy spectrum distortions and the neutral current event rate.

The LSND result [33] which implies

$$\Delta m_{LSND}^2 = (0.2 \div 2) \text{ eV}^2, \quad \sin^2 2\theta_{LSND} = (0.2 \div 4) \cdot 10^{-2} \quad (28)$$

is considered as the most ambiguous hint for neutrino oscillations. The KARMEN [34] experiment does not confirm the LSND result but it also does not fully exclude this result (see [33]). The oscillation interpretation of the LSND result will be checked by the MINIBOONE [35] experiment. A simultaneous explanation of the LSND result and of the solutions of the solar and atmospheric neutrino problems in terms of neutrino mass and mixing requires the introduction of a forth neutrino. We will discuss the  $4\nu$  schemes in section 7.

Summarizing, there is a triple uncertainty affecting predictions of  $m_{ee}$ :

1. An uncertainty in oscillation parameters. The oscillation pattern does not determine uniquely the  $0\nu\beta\beta$ -mass. Moreover, not all relevant oscillation parameters are known, so that additional assumptions are needed.
2. An uncertainty in the absolute scale  $m_1$ . Some information on  $m_1$  can be obtained from cosmology and may be from direct kinematical measurements.
3. An uncertainty in the relative phases. Clearly, the dependence on the phases is small in the case if one of the eigenstates gives a dominating contribution to  $m_{ee}$ .

In what follows we will consider predictions for the  $0\nu\beta\beta$ -mass in schemes of neutrino masses and mixings which explain the solar and the atmospheric neutrino data. The schemes differ by the solution of the solar neutrino problem, the type of the hierarchy and the level of degeneracy. Relative phases are considered as free parameters.

### 3 Schemes with normal mass hierarchy

In the case of strong mass hierarchy,

$$m_1^2 \ll \Delta m_{21}^2 \ll \Delta m_{31}^2, \quad (29)$$

the absolute mass values of the two heavy neutrinos are completely determined by the mass squared differences:

$$m_3^2 = \Delta m_{31}^2 = \Delta m_{atm}^2, \quad m_2^2 = \Delta m_{21}^2 = \Delta m_{\odot}^2. \quad (30)$$

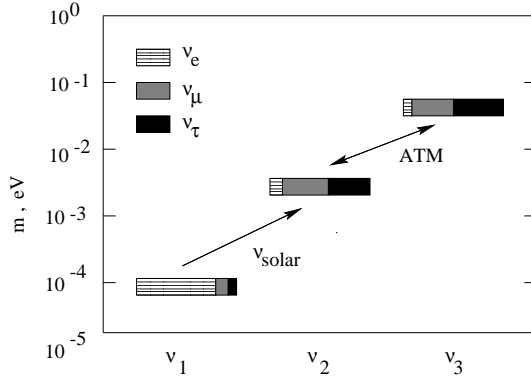


Figure 3: Pattern of neutrino masses and mixing in the scenario with mass hierarchy and SMA solution of the solar neutrino problem. The boxes correspond to mass eigenstates, the sizes of different regions in the boxes show admixtures of different flavors. Weakly hatched regions correspond to the electron flavor, strongly hatched regions depict the muon flavor, black regions present the tau flavor.

The only freedom left is the choice of the value of  $m_1$ . In this case the  $0\nu\beta\beta$ -mass is to a large extent determined by the oscillation parameters.

Since the heaviest neutrino has a mass  $m_3 \leq 0.1$  eV, the neutrino contribution to the Hot Dark Matter component of the universe is small:  $\Omega_\nu < 0.01$ . This neutrino contribution cannot be seen with present and future experimental sensitivity in the CMB radiation, unless a large lepton asymmetry exists [36]. Observational evidence of a significant amount of the HDM component  $\Omega_\nu \gg 0.01$  would testify against this scenario.

### 3.1 Single maximal (large) mixing

In this scheme  $\nu_\mu$  and  $\nu_\tau$  are mixed strongly in  $\nu_2$  and  $\nu_3$  (see fig. 3). The electron flavor is weakly mixed: it is mainly in  $\nu_1$  with small admixtures in the heavy states. The solar neutrino data are explained by  $\nu_e \rightarrow \nu_\mu, \nu_\tau$  resonance conversion inside the Sun. (Notice that  $\nu_e$  converts to  $\nu_\mu$  and  $\nu_\tau$  in comparable portions.) A small admixture of  $\nu_e$  in  $\nu_3$  can lead to resonantly enhanced oscillations of  $\nu_e$  to  $\nu_\tau$  in the matter of the Earth.

Let us consider the contributions to  $m_{ee}$  from individual mass eigenstates. The contribution from the third state,  $m_{ee}^{(3)}$ , can be written in terms of oscillation parameters as

$$m_{ee}^{(3)} \simeq \frac{1}{4} \sqrt{\Delta m_{atm}^2} \sin^2 2\theta_{ee}, \quad (31)$$

where the mixing  $\sin^2 2\theta_{ee} \approx 4|U_{e3}|^2$  determines the oscillations of  $\nu_e$  driven by the atmospheric  $\Delta m_{atm}^2$ . The parameter  $\sin^2 2\theta_{ee}$  immediately gives the depth of oscillation of the  $\nu_e$ -survival probability and it is severely constrained by the CHOOZ experiment. In fig. 4 the iso-mass lines of equal  $m_{ee}^{(3)}$  in the oscillation parameter space are shown, together with various bounds from existing and future reactor and accelerator oscillation experiments. The shaded region shows the favored range of  $\Delta m_{13}^2$  from the atmospheric

neutrino data. As follows from fig. 4 in the Super-K favored region the CHOOZ bound leads to

$$m_{ee}^{(3)} < 2 \cdot 10^{-3} \text{ eV}. \quad (32)$$

For the best fit value of the atmospheric neutrinos the bound is slightly stronger:  $m_{ee}^{(3)} < 1.5 \cdot 10^{-3} \text{ eV}$ .

The mixing  $\sin^2 2\theta_{ee}$  and therefore  $m_{ee}$  can be further restricted by searches of  $\nu_\mu \leftrightarrow \nu_e$  oscillations in the long baseline (LBL) experiments (K2K, MINOS, CERN-Gran-Sasso). The effective mixing parameter measured in these experiments equals  $\sin^2 2\theta_{e\mu} = 4|U_{e3}|^2|U_{\mu 3}|^2$ , so that

$$\sin^2 2\theta_{ee} = \frac{\sin^2 2\theta_{e\mu}}{|U_{\mu 3}|^2}, \quad (33)$$

where the matrix element  $|U_{\mu 3}|^2$  is determined by the dominant mode of the atmospheric neutrino oscillations. Using Eq. (33), the value  $|U_{\mu 3}|^2 = 1/2$  and the expected sensitivity to  $\sin^2 2\theta_{e\mu}(\Delta m^2)$  of K2K and MINOS experiments, we have constructed corresponding bounds in fig. 4. According to fig. 4, these experiments will be able to improve the bound on  $m_{ee}^{(3)}$  by a factor of 2 - 5 depending on  $\Delta m^2$  and reach  $2 \times 10^{-4} \text{ eV}$  for a value of  $\Delta m_{atm}^2$  at the present upper bound. For smaller values of  $|U_{\mu 3}|^2$  the bound on  $m_{ee}$  will be weaker. Taking the smallest value  $|U_{\mu 3}|^2 = 0.3$  allowed by the atmospheric neutrino data, we get that the bound on  $m_{ee}$  will be 1.7 times weaker. In any case, future LBL experiments will be able to probe the whole region of sensitivity of even the second stage of the GENIUS experiment.

A much stronger bound on  $m_{ee}^{(3)}$  can be obtained from studies of neutrino bursts from Supernovae [37]. A mixing parameter as small as  $\sin^2 2\theta_{ee} = 10^{-4}$  can give an observable effect in the energy spectra of supernova neutrinos. This corresponds to  $m_{ee}^{(3)} \sim 2 \cdot 10^{-6} \text{ eV}$ .

The contribution from the second mass eigenstate is completely determined by the parameters being responsible for the solution of the solar neutrino problem:

$$m_{ee}^{(2)} \simeq \frac{1}{4} \sqrt{\Delta m_\odot^2} \sin^2 2\theta_\odot. \quad (34)$$

Taking the 99 % C.L. region of solution (24) we obtain

$$m_{ee}^{(2)} = (5 \cdot 10^{-7} \div 10^{-5}) \text{ eV}, \quad (35)$$

and in the best fit point

$$m_{ee}^{(2)} = 4 \cdot 10^{-6} \text{ eV}. \quad (36)$$

The contribution from the lightest state is

$$m_{ee}^{(1)} = m_1 \cos^2 \theta_\odot \simeq m_1 \ll m_2 < 2 \cdot 10^{-3} \text{ eV}, \quad (37)$$

which can be even larger than  $m_{ee}^{(2)}$ : if the hierarchy between the masses of the first and the second state is not too strong,  $m_1/m_2 > 10^{-2}$  (for comparison  $m_e/m_\mu = 5 \cdot 10^{-3}$ ), we

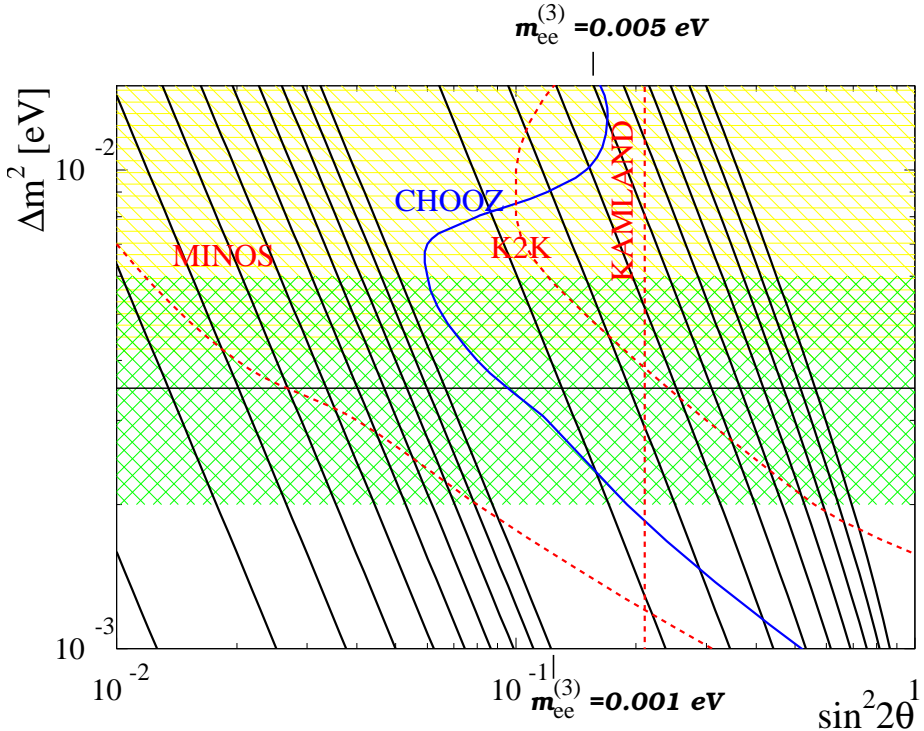


Figure 4: Iso-mass ( $|m_{ee}^{(3)}|$ ) lines (solid lines) in the scheme with hierarchical mass spectrum. From the upper right downward  $|m_{ee}^{(3)}|$  decreases from 0.005 eV to 0.0001 eV. Also shown are the regions favored by the Super-Kamiokande atmospheric neutrino data with current bestfit (solid horizontal line) and Kamiokande (lower and upper shaded areas, respectively, according to [29]) and the borders of the regions excluded by CHOOZ (solid line) [38] as well as the expected final sensitivity of KAMLAND and K2K (dashed) [39] as well as of MINOS [40].

get  $m_{ee}^{(1)} > 2 \cdot 10^{-5}$  eV, with a typical interval  $m_{ee}^{(1)} \sim (0.2 - 2) \cdot 10^{-4}$  eV.

Summing up the contributions (see fig. 5) one finds a maximal value for the  $0\nu\beta\beta$ -mass

$$m_{ee}^{max} = (2 - 3) \cdot 10^{-3} \text{ eV} \quad (38)$$

which is dominated by the third mass eigenstate. No lower bound on  $m_{ee}$  can be obtained from the present data. Indeed,  $U_{e3}$  and therefore  $m_{ee}^{(3)}$  can be zero. The same statement is true for  $m_{ee}^{(1)}$ , since no lower bound for  $m_1$  exists. The only contribution bounded from below is  $m_{ee}^{(2)} > 10^{-6}$  eV. However, cancellations with the two other states can yield a zero value for the total  $m_{ee}$  (see fig. 5).

The following conclusions on future double beta experiments and neutrino oscillations can be drawn

- 1). If future experiments will detect neutrinoless beta decay with a rate corresponding to  $m_{ee} > 2 \cdot 10^{-3}$  eV, the scenario under consideration will be excluded, unless contributions

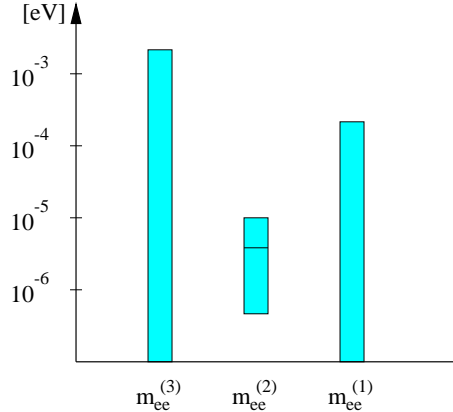


Figure 5: Contributions to  $m_{ee}$  from the individual mass eigenstates for the single maximal mixing scheme with mass hierarchy. The bars correspond to allowed regions.

to  $0\nu\beta\beta$  decay from alternative mechanisms exist.

2). As we have pointed out, future long-baseline oscillation experiments on  $\nu_\mu \rightarrow \nu_e$  oscillations (MINOS) may further improve the bound on  $U_{e3}^2$  and therefore on  $m_{ee}^{max}$  by a factor of  $\sim 2 - 5$ . A much stronger bound may be obtained from supernovae studies [37]. As follows from fig. 4 and from the fact the SMA solution is realized, KAMLAND should give a zero-result in this scheme.

3). An important conclusion can be drawn if future LBL and atmospheric neutrino experiments will observe  $\nu_e$ -oscillations near the present upper bound. In particular, an up-down asymmetry of the  $e$ -like events at Super-Kamiokande is one of the manifestations of these oscillations [41]. In this case the  $\nu_3$  contribution to  $m_{ee}$  dominates, no significant cancellation is expected and the dependence on the relative phases is weak. One predicts then the result

$$m_{ee} \approx m_{ee}^{(3)} \sim U_{e3}^2 \sqrt{\Delta m_{atm}^2}. \quad (39)$$

The observation of  $0\nu\beta\beta$  decay with  $m_{ee}^{exp} \sim m_{ee}^{(3)}$  would provide a strong evidence of the scheme, provided that the SMA solution will be established. On the other hand it will be difficult to exclude the scheme if  $0\nu\beta\beta$  decay will not be observed at the level which corresponds to  $m_{ee}$  (39). In this case the scheme will be disfavored. However one should take into account also possible cancellations of  $m_{ee}^{(3)}$  and  $m_{ee}^{(1)}$ , if the mass hierarchy is weak.

### 3.2 Bi-large mixing

The previous scheme can be modified in such a way that the solar neutrino data are explained by the large angle MSW conversion. Now the  $\nu_e$  flavor is strongly mixed in  $\nu_1$  and  $\nu_2$  (see fig. 6).

The contribution from the third state is the same as in the previous scheme (see eq. (31)) with the upper bound  $m_{ee}^{(3)} < 2 \cdot 10^{-3}$  eV (32).

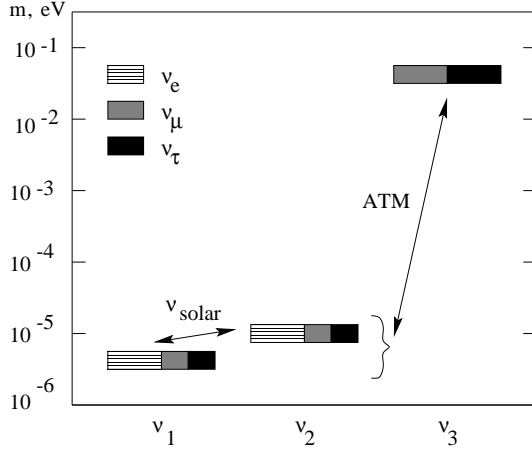


Figure 6: Neutrino masses and mixing pattern of the bi-maximal mixing scheme with mass hierarchy.

The contribution from the second level,

$$m_{ee}^{(2)} = \frac{1}{2} \left( 1 - \sqrt{1 - \sin^2 2\theta_{\odot}} \right) \sqrt{\Delta m_{\odot}^2} , \quad (40)$$

can be significant: both the mixing parameter and the mass are now larger. According to fig. 7, in the region of the LMA solution of the solar neutrino problem, the contribution can vary in the interval

$$m_{ee}^{(2)} = (0.5 - 4) \cdot 10^{-3} \text{ eV} . \quad (41)$$

In the best fit point we get  $m_{ee}^{(2)} \simeq 1.4 \cdot 10^{-3} \text{ eV}$ . Notice that a lower bound on  $m_{ee}^{(2)}$  exists in this scheme, provided that  $\sin^2 2\theta < 1$ . Notice that a day-night asymmetry of about 6 % indicated by the Super-Kamiokande experiment would correspond to  $m_{ee}^{(3)} = (1 - 3) \cdot 10^{-3} \text{ eV}$ .

The contribution  $m_{ee}^{(1)}$ :

$$m_{ee}^{(1)} \simeq \cos^2 \theta_{\odot} m_1 , \quad (42)$$

where  $\cos^2 \theta \simeq 0.5 - 0.84$ , is smaller than in the previous scheme of sect. 3.1, since now  $\nu_e$  is not purely  $\nu_1$  and  $m_1$  can be as large as  $1 \cdot 10^{-3} \text{ eV}$  for  $m_1/m_2 < 0.1$ . Due to the mass hierarchy  $m_{ee}^{(1)}$  is much smaller than  $m_{ee}^{(2)}$  (see fig. 8).

Summing up the contributions, we get a maximal value of  $m_{ee}^{max} \simeq 7 \cdot 10^{-3} \text{ eV}$ . The typical expected value for  $m_{ee}$  is in the range of several  $10^{-3} \text{ eV}$ . However, no lower bound on  $m_{ee}$  can be obtained on the basis of the present data, although values of  $m_{ee}$  being smaller than  $10^{-3} \text{ eV}$  require some cancellation of the contributions  $m_{ee}^{(2)}$  and  $m_{ee}^{(3)}$ .

Let us consider possible implications of future results from oscillations and  $0\nu\beta\beta$  decay searches:

- The observation of  $m_{ee} > (\text{few}) \cdot 10^{-2} \text{ eV}$  will exclude the scheme.

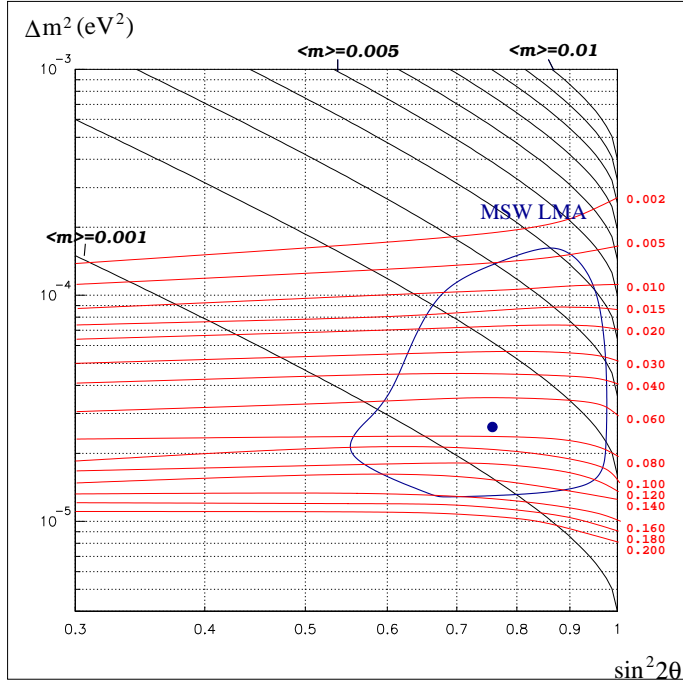


Figure 7: The iso-mass  $m_{ee}^{(2)}$  lines, determining the contribution of the second state in the  $\Delta m_{12}^2 - \sin^2 2\theta_{12}$  plane for the hierarchical scheme with the LMA MSW solution. From the upper right downward:  $|m_{ee}^{(2)}|$  decreases from 0.01 to 0.001 eV. Also shown is the MSW LMA 99 % C.L. allowed region from the combined analysis of the Homestake, Gallex, Sage and Super-Kamiokande rates and the Super-Kamiokande and the day-night asymmetry at Super-Kamiokande. The point indicates the best fit value parameters. The horizontal lines correspond to contours of constant day-night asymmetry [42]. KAMLAND should observe a disappearance signal in this model.

- The non-observation of  $0\nu\beta\beta$  decay will not exclude the scheme due to possible cancellations.

The situation can, however, change in the future, if oscillation experiments restrict strongly one of the contributions  $m_{ee}^{(2)}$  or  $m_{ee}^{(3)}$ . Let us discuss possible developments in this direction:

- Within several years solar neutrino experiments will check the LMA-solution. In particular, further measurements of the day-night asymmetry and zenith angle distribution at Super-K and SNO could give a decisive identification of the solution of the solar neutrino problem (see fig. 7). Notice that precise measurements of the day/night asymmetry can sharpen the predictions of  $m_{ee}^{(2)}$ . Moreover, the LBL reactor experiment KAMLAND should observe an oscillation effect thus providing an independent check of the LMA MSW solution.
- If MINOS or atmospheric neutrino studies will fix  $m_{ee}^{(3)}$  near the present upper bound,

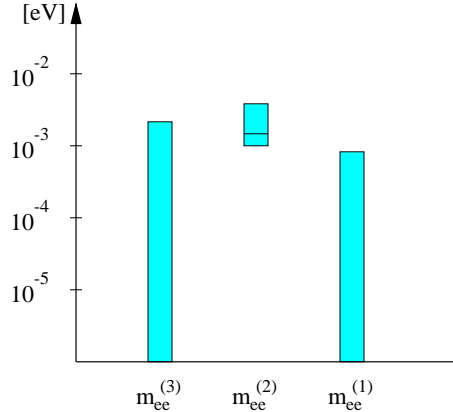


Figure 8: Contributions from different mass eigenstates to  $m_{ee}$  for the bi-large mixing scheme with mass hierarchy.

one can study the interference effects of  $m_{ee}^{(2)}$  and  $m_{ee}^{(3)}$  in  $0\nu\beta\beta$  decay determined by the relative phases  $\phi_2$  and  $\phi_3$ .

### 3.3 Scheme with Vacuum oscillation solution

The solar electron neutrinos  $\nu_e$  oscillate in vacuum into comparable mixtures of  $\nu_\mu$  and  $\nu_\tau$ . The fit to the data indicates several disconnected regions in the  $\Delta m^2 - \sin^2 2\theta$  - plot. We consider the large  $\Delta m^2$  region,  $\Delta m^2 = (4 - 9) \cdot 10^{-10} \text{ eV}^2$ , and  $\sin^2 2\theta > 0.8$ , where oscillations allow one to explain an excess of the e-like events in the recoil electron spectrum indicated by Super-Kamiokande. (Obviously a small  $\Delta m^2$  will give even smaller contributions to the effective Majorana mass). In this case

$$m_{ee}^{(2)} = \sqrt{\Delta m^2} \sin^2 \theta_\odot < 2 \cdot 10^{-5} \text{ eV}. \quad (43)$$

Due to the mass hierarchy and large mixing, the lightest mass eigenstate gives an even smaller contribution:  $m_{ee}^{(1)} \ll m_{ee}^{(2)}$ . The contribution from the third state is the same as in Eq. (31) and in fig. 4. For the sum we get

$$m_{ee} \simeq m_{ee}^{(3)} < 2 \cdot 10^{-3} \text{ eV}, \quad (44)$$

and clearly,  $m_{ee}^{(3)}$  can be the dominant contribution (fig. 9).

The following conclusions may be drawn:

- 1). The observation of  $m_{ee} > 10^{-2}$  eV will exclude the scheme. On the other hand there is no minimal value for  $m_{ee}$  according to the present data, so that negative results of searches for  $0\nu\beta\beta$  decay will have no serious implications for this scheme.
- 2) A positive signal for atmospheric  $\nu_e$  oscillations or in the MINOS experiment will allow us to predict uniquely the value of  $m_{ee}$ . Then searches for  $m_{ee}$  will give a crucial check of the scheme. The absolute scale of the neutrino mass will be fixed.

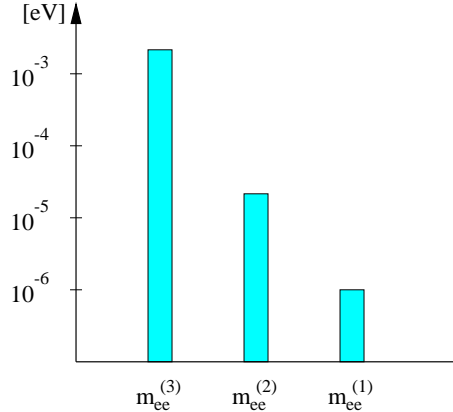


Figure 9: Contributions from different mass eigenstates to  $m_{ee}$  for the bi-maximal mixing scheme with mass hierarchy.

Similar results can be obtained for the LOW MSW solution. Here the mass squared difference  $\Delta m_{21}^2 = 3 \cdot 10^{-7} \text{ eV}^2$  implies

$$m_{ee}^{(2)} < 3 \cdot 10^{-4} \text{ eV}. \quad (45)$$

Again  $m_{ee}^{(1)} \ll m_{ee}^{(2)}$ , and the main contribution may arise from the third state.

Thus, models with normal mass hierarchy lead to rather small values of  $m_{ee}$ , certainly below  $10^{-2} \text{ eV}$ . Moreover, the largest value can be obtained in the scheme with the LMA MSW solution of the solar neutrino problem. The lower bound is of the order  $\sim 10^{-3} \text{ eV}$ , unless cancellation (which looks rather unnatural) occurs. Clearly, only the second stage of the GENIUS experiment can obtain positive results.

### 3.4 Triple maximal mixing scheme

In the scheme of [43] all elements of the mixing matrix are assumed to be equal:  $|U_{ij}| = 1/\sqrt{3}$  (see fig. 10). The  $0\nu\beta\beta$ -mass is dominated by the contribution from the third state:

$$m_{ee}^{(3)} = \frac{1}{3} \sqrt{\Delta m_{atm}^2}. \quad (46)$$

The best fit of the atmospheric neutrino data in this scheme implies that  $\Delta m_{atm}^2 \simeq 8 \cdot 10^{-4} \text{ eV}^2$  and thus

$$m_{ee} \approx 10^{-2} \text{ eV}. \quad (47)$$

The scheme has rather definite predictions for solar and atmospheric neutrinos. It does not give a good fit of the data and will be tested by forthcoming experiments.

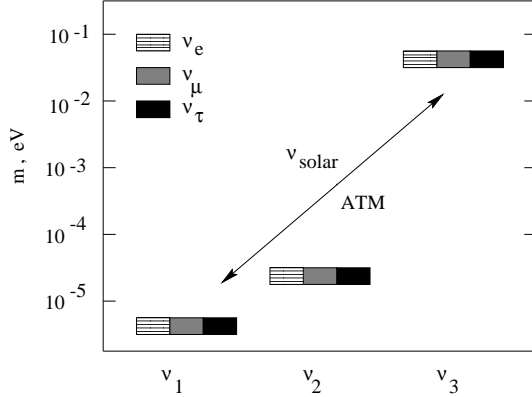


Figure 10: Neutrino masses and mixing in the scheme with threefold maximal mixing.

## 4 Schemes with partial degeneracy

In the case of partial mass degeneracy,

$$\Delta m_{21}^2 \ll m_1^2 \ll \Delta m_{31}^2 , \quad (48)$$

the masses of the two light neutrinos are approximately equal to  $m_1$  and the heaviest mass is determined by the atmospheric mass squared difference:

$$m_1 \approx m_2, \quad m_3 \approx \sqrt{\Delta m_{31}^2} = \sqrt{\Delta m_{atm}^2} . \quad (49)$$

The interval of masses implied by the condition of partial degeneracy (48) is rather narrow especially for the LMA and SMA solutions of the solar neutrino problem, when  $\Delta m_{31}^2$  and  $\Delta m_{21}^2$  differ by two orders of magnitude only. A mass value of  $m_1 > 3 \cdot 10^{-2}$  eV will shift  $m_3$  to larger values, and therefore influence the contribution from the third eigenstate. We will consider this ‘‘transition’’ case separately in sect. 6.

The contribution from the third state is the same as in hierarchical schemes (see fig. 4). For the two light states, the contribution can be written as

$$m_{ee}^{(1)} + m_{ee}^{(2)} \simeq m_1 (\cos^2 \theta_\odot + e^{i\phi_2} \sin^2 \theta_\odot) , \quad (50)$$

and depending on the relative phase  $\phi_2$  it varies in the interval

$$m_{ee}^{(1)} + m_{ee}^{(2)} = m_1 (\cos 2\theta_\odot - 1) . \quad (51)$$

This contribution can be further restricted, if the solution of the solar neutrino problem will be identified. In the case of the SMA MSW solution  $m_{ee}^{(1)}$  dominates; the dependence on the phase practically disappears and one gets

$$m_{ee}^{(1)} + m_{ee}^{(2)} \simeq m_1 . \quad (52)$$

The condition of partial degeneracy implies that the mass  $m_1$  should be in the interval:

$$0.5 \cdot 10^{-2} \text{ eV} < m_1 < 3 \cdot 10^{-2} \text{ eV} ,$$

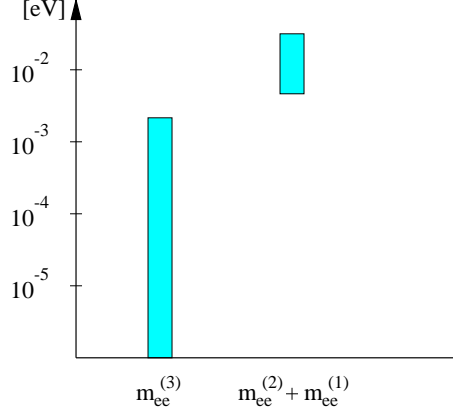


Figure 11: Contributions from different mass eigenstates to  $m_{ee}$  for partially degenerate scenarios with MSW SMA solution.

and therefore,  $m_1$  can reach  $3 \cdot 10^{-2}$  eV at most (fig. 11).

Summing up all contributions we expect  $m_{ee}$  between  $10^{-3}$  and  $3 \cdot 10^{-2}$  eV. Notice that a lower bound on  $m_{ee}$  exists here. Near the upper bound the mass  $m_{ee}$  is dominated by the contribution from the lightest states and therefore the  $0\nu\beta\beta$  decay rate will give a direct measurement of  $m_1$ :  $m_1 \approx m_{ee}$ .

Observations of  $m_{ee}$  larger than  $m_{ee}^{(3)} = U_{e3}^2 m_3$  ( $m_{ee}^{(3)}$  can be determined from oscillation experiments) by oscillation experiments) would favor the scheme, although will not allow one to identify it unambiguously.

Future observations of  $0\nu\beta\beta$  decay with  $m_{ee} > 3 \cdot 10^{-2}$  eV will exclude the scheme testifying for spectra with complete degeneracy or inverse hierarchy (see sect. 5 or 7).

For the LMA solution the typical  $\Delta m_{21}^2$  is bigger than in the SMA case and the condition of partial degeneracy implies an even narrower interval  $m_1 = (1 - 3) \cdot 10^{-2}$  eV. Moreover, for  $m_1$  at the lower limit of this interval, the difference of light mass eigenvalues can give a substantial correction to formula (50). In the lowest approximation of  $\frac{\Delta m^2}{m_1^2}$  we get:

$$m_{ee}^{(1)} + m_{ee}^{(2)} \simeq m_1 (\cos^2 \theta_\odot + e^{i\phi_2} \sin^2 \theta_\odot) + e^{i\phi_2} \frac{\Delta m_\odot^2}{2m_1} \sin^2 \theta_\odot. \quad (53)$$

The correction (last term in this equation) can be as big as  $10^{-3}$  eV and may turn out to be important when a cancellation of  $m_{ee}^{(1)}$  and  $m_{ee}^{(2)}$  occurs.

Summing up the contributions we find, that the maximal value of  $m_{ee}$  can be about  $3 \cdot 10^{-2}$  eV as in the case of the SMA solution with similar implications for future  $0\nu\beta\beta$  decay searches. In contrast with the SMA case, now due to possible strong cancellations of the contributions no lower bound on  $m_{ee}$  can be obtained from the present data (fig.12).

Future oscillation results will allow to sharpen the predictions of  $m_{ee}$ . In particular, the solar neutrino experiments will allow to measure a deviation of mixing from the maximal value. The bound  $1 - \sin^2 2\theta_\odot > 0.1$  would imply that  $m_{ee}^{(1)} + m_{ee}^{(2)} > 3 \cdot 10^{-3}$  eV. In this case no complete cancellation in  $m_{ee}$  is possible and a minimum value  $m_{ee} \geq 10^{-3}$

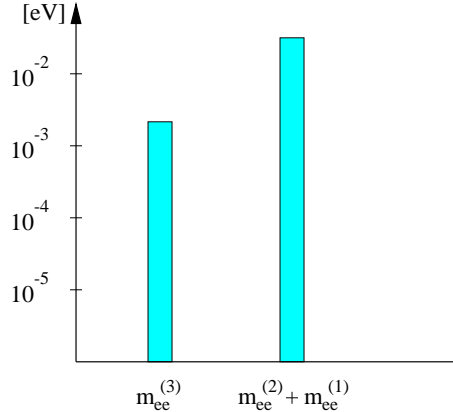


Figure 12: Contributions to  $m_{ee}$  from different mass eigenstates in schemes with partial degeneracy and LMA, LOW or VO solutions of the solar neutrino problem. The degenerate states give the main contribution. A complete cancellation of contributions is possible.

eV appears. The searches for  $\nu_e$ -oscillations driven by  $\Delta m_{atm}^2$  will further restrict (or measure)  $m_{ee}^{(3)}$ .

Future studies of the  $0\nu\beta\beta$  decay can have the following implications: (i) A measurement of  $m_{ee} > 2 \cdot 10^{-2}$  eV will exclude the scheme. (ii) The non-observation of  $m_{ee}$  at the level of  $10^{-3}$  eV (second stage of GENIUS) can exclude the scheme if future oscillation experiments will lead to a determination of the sum  $m_{ee}^{(1)} + m_{ee}^{(2)}$  and a lower bound on  $m_{ee}$  will be derived. (iii) If  $m_{ee}$  will be observed at the level  $(0.3 - 2)10^{-2}$  eV (and alternative schemes which yield a prediction in this interval will be rejected by other observations), then  $m_{ee}$  measurements will imply a certain bound in the  $m_1 - \phi_2$  plane.

In the case of the LOW solution  $\Delta m_{\odot}^2$  is much smaller than for the LMA solution and  $m_1$  can be in the interval  $m_1 = (10^{-3} - 3 \cdot 10^{-2})$  eV. Correspondingly, the contribution from the two lightest states can be in the wider range  $(10^{-4} - 3 \cdot 10^{-2})$  eV. The maximal value for  $m_{ee}$  can reach  $3 \cdot 10^{-2}$  eV. However it will be impossible to establish a lower bound on  $m_{ee}$  even if the solar mixing angle  $\theta_{\odot}$  will be measured.

Notice that the LOW solution can be identified by a specific enhancement of the regeneration effects (in particular the day/night asymmetry) in the lower energy part of the solar neutrino spectrum. An especially strong effect is expected on the  ${}^7Be$ -line.

For vacuum oscillations the situation is similar to the LOW case.

## 5 Schemes with complete mass degeneracy

In schemes with a degenerate neutrino mass spectrum the common mass  $m_1$  is much larger than the mass splittings:

$$\Delta m_{21}^2 \ll \Delta m_{31}^2 \ll m_1^2. \quad (54)$$

This can be realized as long as  $m_1 > 0.1$  eV.

Already the present bound  $m_{ee} < 0.2 - 0.4$  eV [44] implies not too strong degeneracy unless a substantial cancellation of the contributions in  $m_{ee}$  occurs. Indeed, if  $\Delta m_{atm}^2 = 3 \cdot 10^{-3}$  eV<sup>2</sup>, and  $m_1 \sim 0.2$  eV, we get

$$\frac{\Delta m_{23}}{m_1} \approx \frac{\Delta m_{atm}^2}{2m_2^2} = 4 \cdot 10^{-2}. \quad (55)$$

For  $m_1 = 0.1$  eV, the ratio equals 0.15.

In the case of the SMA solution the  $\nu_e$  flavor is mainly concentrated in  $\nu_1$  and

$$m_{ee}^{(1)} \simeq m_1 \cos^2 \theta_\odot \gg m_{ee}^{(2)} \gg m_{ee}^{(3)}. \quad (56)$$

Numerically, we get  $m_{ee} \sim m_{ee}^{(1)} \sim m_1 > 0.1$  eV, *i.e.* close to the present bound. Basically one measures  $m_1$  by measuring the  $0\nu\beta\beta$ -mass (see fig. 13).

Important conclusions follow from a comparison of the  $0\nu\beta\beta$  decay results with the cosmological bounds on the neutrino mass [20], as well as from bounds which follow from observations of the large scale structure of the Universe. In this scenario one expects

$$\sum m_i = 3m_{ee}, \quad (57)$$

and therefore

$$\Omega_\nu = \frac{3m_{ee}}{91.5 \text{eV}} h^{-2}. \quad (58)$$

Thus the effective Majorana mass,  $\Omega_\nu$  and the Hubble constant are related. This relation may have the following implications:

1). A significant deviation from equation (58) will exclude the scheme. The present bound on  $m_{ee}$  implies  $3m_1 \leq (0.6 - 1)$  eV. If, *e.g.*, data on the large scale structure of the universe will require  $\sum m_i \simeq 1$  eV, this scheme will be excluded [15, 17].

2). The discovery of  $0\nu\beta\beta$  decay at the level of the present bound, 0.1 - 0.2 eV, will give  $\sum m_i \simeq 0.3 - 0.6$  eV. This range can be probed by MAP and Planck. If these experiments will put a bound on the sum of neutrino masses below 0.3 eV the scheme will be excluded.

3). This scheme will also be excluded, if cosmological observations will require  $\sum m_i > 0.3$  eV, but  $0\nu\beta\beta$  decay searches will give a bound below  $m_{ee} < 0.1$  eV, the scheme will be excluded.

Apart from a confirmation of the SMA solution future oscillation experiments will not influence predictions of  $m_{ee}$  in this scheme.

Observations of  $m_{ee}$  at the level 0.1 - 0.4 eV will be in favor of the scheme.

For the LMA solution a significant cancellation of the contributions from the first and the second state may occur, resembling the situation in the partially degenerate case. We have

$$m_{ee}^{(1)} + m_{ee}^{(2)} \simeq m_1(\cos^2 \theta_\odot + e^{i\phi_2} \sin^2 \theta_\odot), m_{ee}^{(3)} = m_1 |U_{e3}|^2. \quad (59)$$

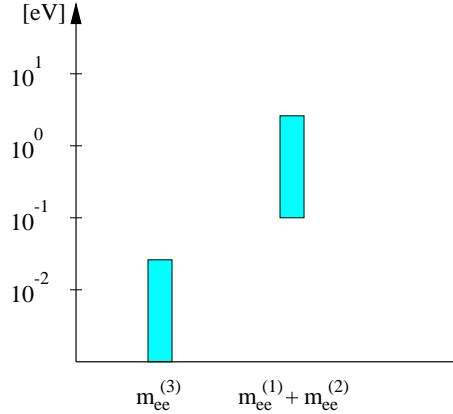


Figure 13: Contributions from different mass eigenstates to  $m_{ee}$  for the scenario with complete mass degeneracy and the SMA solution of the solar neutrino problem.

Since  $U_{e3}^2 \leq 0.03$ , the contribution from the first two states dominates (fig. 15), unless strong mixing, which has an extremely small deviation from maximal mixing, is introduced:  $|1 - \sin^2 2\theta_\odot| < 10^{-3}$ , which leads to strong cancellation. Thus

$$m_{ee} \approx m_{ee}^{(1)} + m_{ee}^{(2)} = (\cos 2\theta_\odot - 1) \cdot m_1 = (0.2 - 1)m_1 , \quad (60)$$

and since  $m_1 > 0.1$  eV, we expect for  $\sin^2 2\theta = 0.96$ :

$$m_{ee} \geq 2 \cdot 10^{-2} \text{ eV}. \quad (61)$$

Notice that some recent studies show that even exact maximal mixing is allowed by the present data, so that the cancellation can be complete.

Precise measurements of  $\theta_\odot$  in future oscillation experiments will play a crucial role for predictions of the mass  $m_{ee}$ .

If the scheme will be identified, measurements of  $m_{ee}$  will provide a bound in the  $m_1 - \phi$ -plane.

The same results hold also for the LOW solution.

For the vacuum oscillations of the  $\nu_\odot$ -problem, the situation is similar to the one with LMA MSW. In the strict bi-maximal scheme  $U_{e3}^2 = 0$  and  $U_{e1}^2 = U_{e2}^2$ , so that  $m_{ee} \equiv 0$  in the limit of equal masses. Small deviations from zero can be related to the mass difference of  $m_1$  and  $m_2$ :

$$m_{ee} \simeq \frac{1}{2}(m_1 - m_2) = \frac{1}{4} \frac{\Delta m_\odot^2}{m_1} \simeq 10^{-10} \text{ eV} \frac{1 \text{ eV}}{m_1}. \quad (62)$$

Thus, no unique prediction for  $m_{ee}$  exists. Although a large value  $m_{ee} > 0.1$  eV would favor degenerate scenarios, the non-observation of  $0\nu\beta\beta$  decay at the level of 0.1 eV will not rule out the scheme.

The identification of the scenario will require (i) a strong upper bound on  $U_{e3}$ , (ii) the confirmation of the vacuum oscillation solution and (iii) a large  $m_{ee} > 0.1$  eV. This would

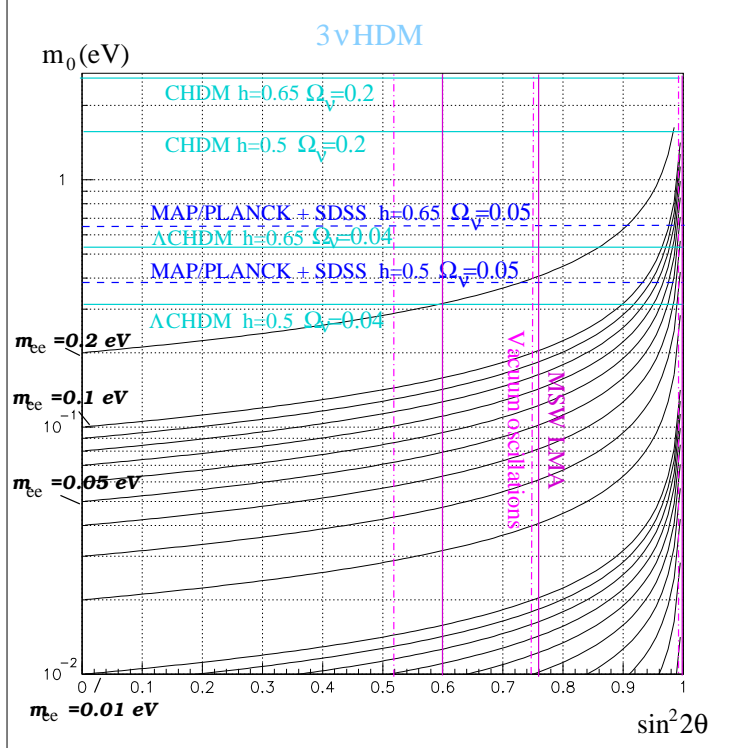


Figure 14: Plotted are iso-mass lines in the  $m_1 - \sin^2 2\theta$  plane for the case of cancellation between the contributions  $m_1$  and  $m_2$  in degenerate scenarios. Mass splitting is neglected, since  $m_2 - m_1 \ll m_1$  and  $m_3 - m_1 < 0.1m_1$ . Shown are the bestfit values of  $m_0$  for cold+hot dark matter (CHDM) (according to [45]) and cosmological-constant+cold+hot dark matter (ΛCHDM) (according to [46]) scenarios for different values of the Hubble constant. Also shown is the sensitivity to  $m_0$  of MAP/Planck combined with SDSS according to [47]. Also shown are the regions of the LMA and VO solutions with best fit line according to [48].

testify for the case of addition of the  $\nu_1$  and  $\nu_2$  contributions. An upper bound on  $m_1$  can be obtained from cosmology.

If however  $0\nu\beta\beta$  decay will not be discovered it will be practically impossible to exclude the scenario (and distinguish it from the hierarchical cases), unless cosmology will be able to measure neutrino masses down to  $m_1 \simeq 0.1$  eV. The key element is the precise determination of  $\theta_\odot$  and its deviation from the maximal mixing.

Let us consider how deviations from the exact bi-maximal case affect the predictions for the rate in double beta decay experiments. The lower bound on the effective mass turns out to be

$$m_{ee} \simeq m_1 \sqrt{1 - \sin^2 2\theta} . \quad (63)$$

We show this result in fig. 14 as lines of minimal values of  $m_{ee}$  in the  $m_1 - \sin^2 2\theta$  plane. These lines give the lower bound on values of  $m_1$  and the upper bound on values of  $\sin^2 2\theta$ .

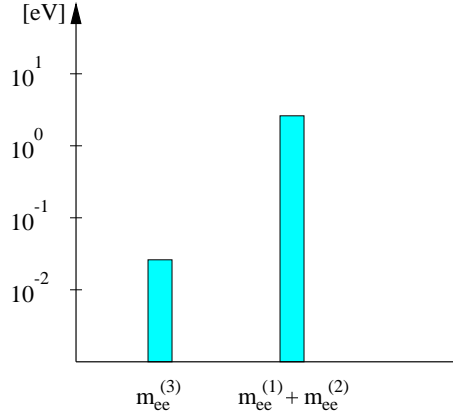


Figure 15: Contributions from different mass eigenstates to  $m_{ee}$  for the scenario with complete degeneracy and LMA, LOW or VO solution.

for which a given value  $m_{ee}$  can be reproduced. We have shown also the favored regions of the solar MSW large mixing angle solution as well as the “Just-so” vacuum oscillation solution. For the bestfit value of the ACHDM model  $m_1 = 0.3$ , a Hubble constant  $h = 0.5$  and the best fit value of the mixing angle  $\sin^2 2\theta = 0.76$  we get from the fig 14  $m_{ee} \simeq 0.2$  eV close to the present experimental bound. Larger mixing allows for smaller values of  $m_{ee}$ . In fig. 14 also shown is the sensitivity of CMB studies with MAP and Planck combined with the Sloan Digital Sky Survey. For not too large mixing already the present  $0\nu\beta\beta$  decay bound obtained from the Heidelberg-Moscow experiment [44] is close to the sensitivity of these cosmological observations.

## 6 Transition regions

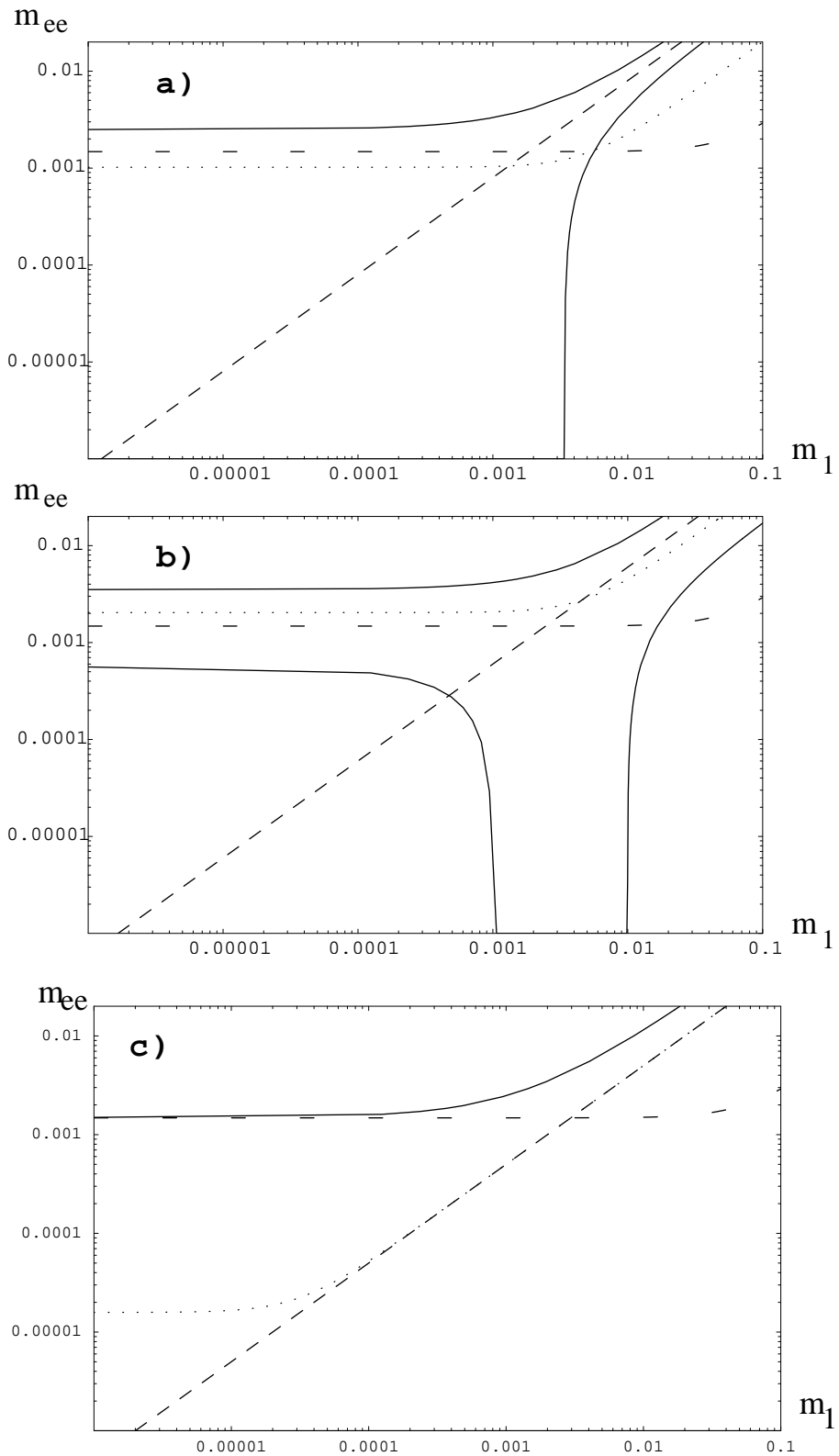
There are two intermediate regions of  $m_1$ :

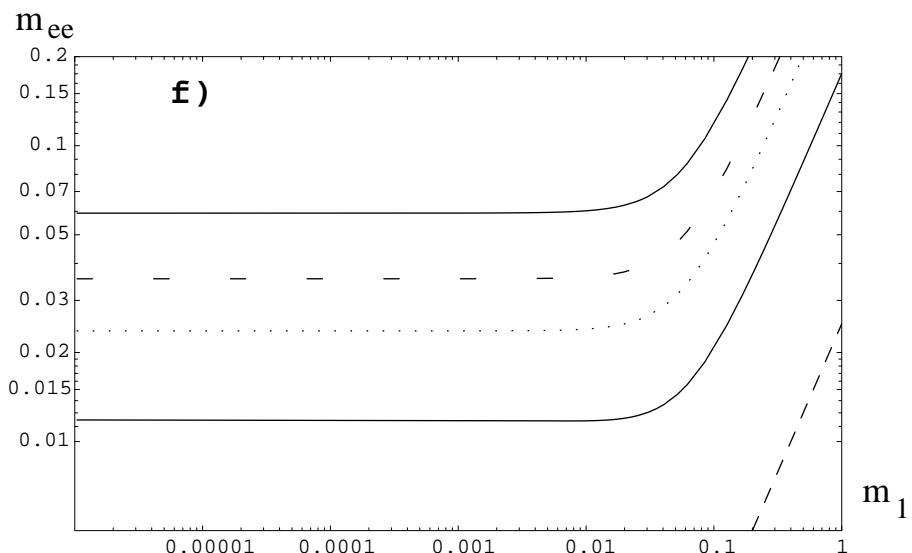
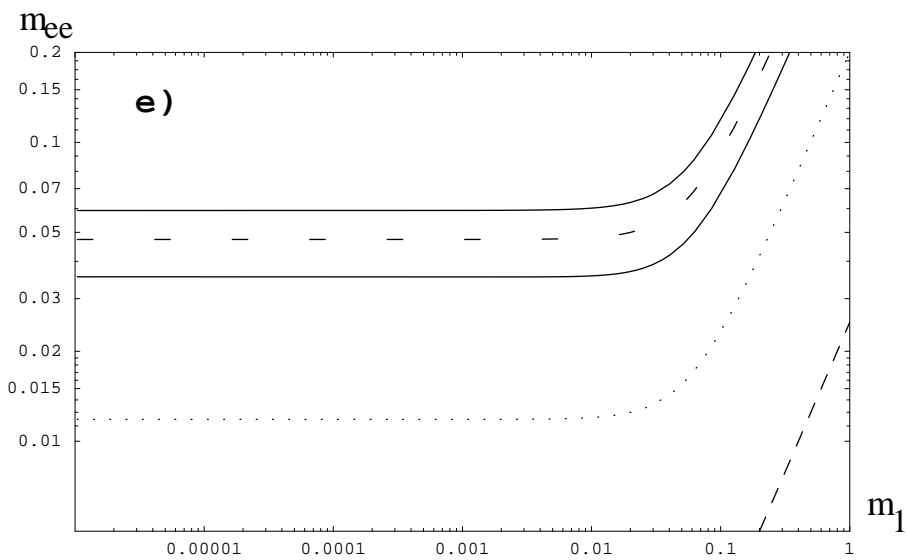
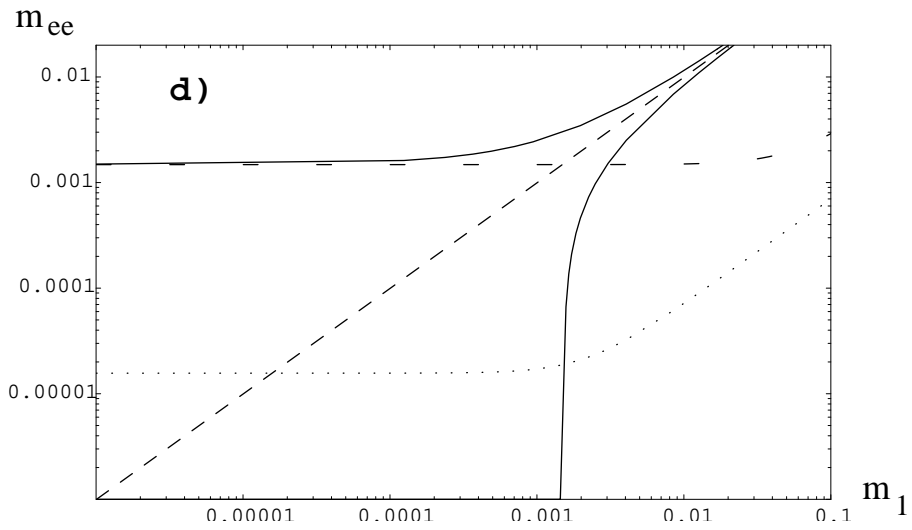
- 1) The region with  $m_1 \sim \sqrt{\Delta m_{\odot}^2}$ , where the transition between the hierarchical case and the case with partial degeneracy occurs. Here  $m_1 \sim m_2 \ll m_3$ .
- 2). The region with  $m_1 \sim \sqrt{\Delta m_{atm}^2}$  which corresponds to the transition between partial degeneracy to complete degeneracy:  $m_1 \approx m_2 \sim m_3$ . Here the two lightest states are strongly degenerate and their contributions are described by eq. (51) in sect. 4. with the only difference that  $m_1$  now can be larger. For  $m_1^2 \sim \Delta m_{atm}^2$ ,  $m_1$  and therefore  $m_{ee}$  can reach 0.1 eV.

The contribution from the third state is also modified:

$$m_{ee}^{(3)} = |U_{e3}|^2 \sqrt{\Delta m_{atm}^2} \left[ 1 + \frac{m_1^2}{\Delta m_{atm}^2} \right]^{1/2}. \quad (64)$$

Thus now for the same values of the oscillation parameters the contribution  $m_{ee}^{(3)}$  can be  $[1 + m_1^2/\Delta m_{atm}^2]^{1/2} \sim (1 - 2)$  times larger.





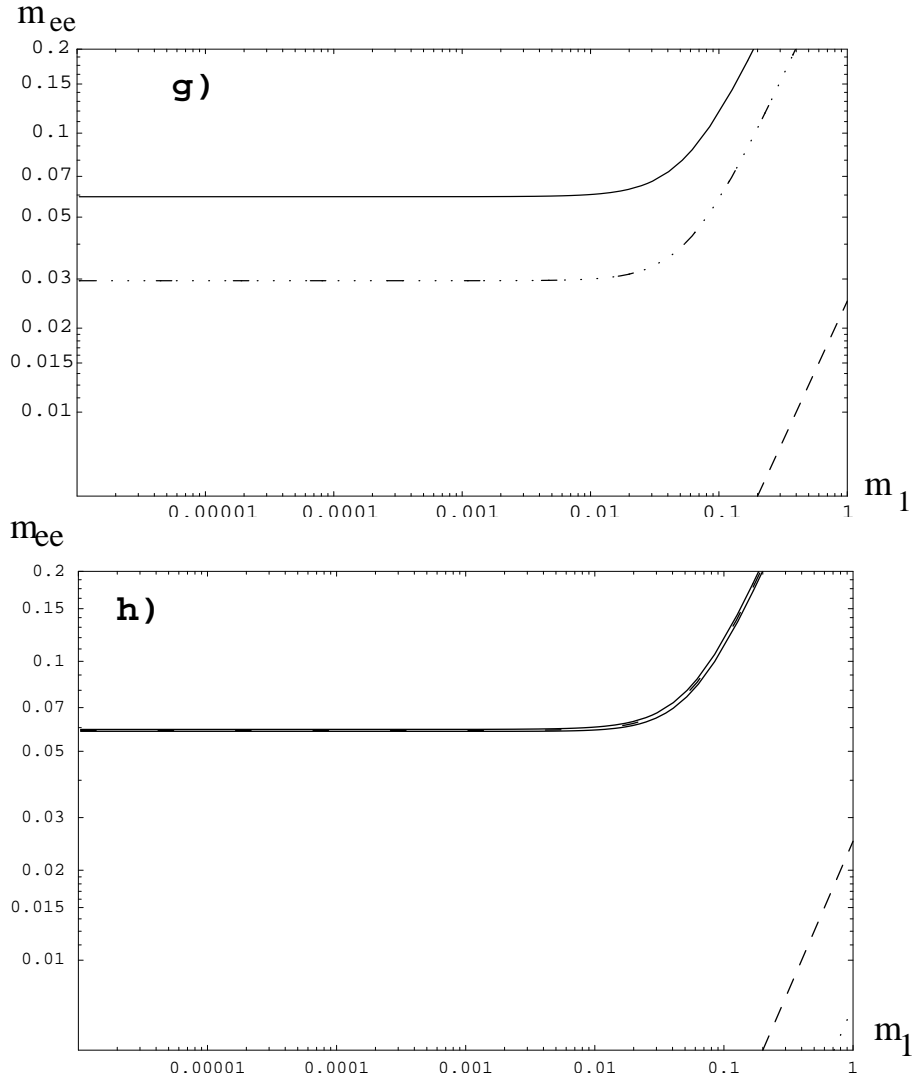


Figure 16:  $m_{ee}$  (eV) as a function of  $m_1$  (eV) for three-neutrino mixing. Shown are the contributions  $m_{ee}^{(1)}$  (dashed),  $m_{ee}^{(2)}$  (dotted) and  $m_{ee}^{(3)}$  (interrupted dashes). The solid lines correspond to  $m_{ee}^{max}$  and  $m_{ee}^{min}$  and show the allowed region for  $m_{ee}$ . Panels a)-d) correspond to the case for normal hierarchy, panels e)-h) – inverse hierarchy. Shown are the cases a) and e) LMA MSW with  $U_{e2}^2 = 0.2$ , b) and f) LMA MSW with  $U_{e2}^2 = 0.4$ , c) and g) vacuum oscillation with  $U_{e2}^2 = 0.5$  and d) and h) SMA MSW with  $U_{e2}^2 = 7 \cdot 10^{-3}$ . The mixing of the third state is varied from zero to its upper bound,  $U_{e3}^2 = 2.5 \cdot 10^{-2}$ .

In fig.16 we show the dependence of the individual contributions to  $m_{ee}$  on  $m_1$ . For  $m_{ee}^{(3)}$  only the upper bound is used; the two other lines represent possible values of  $m_{ee}^{(1)}$  and  $m_{ee}^{(2)}$  for certain neutrino mixing parameters. We show also the maximal and the minimal possible values of  $m_{ee}$ .

The position of the first transition region is determined by the specific solution of the solar neutrino problem: According to fig. 16,  $m_1 = (2 - 15) \cdot 10^{-3}$  eV for the LMA solution,  $m_1 = (1 - 9) \cdot 10^{-3}$  eV for the SMA MSW solution and  $m_1 = (1 - 10) \cdot 10^{-5}$  eV for the VO solution.

The position of the second transition region,  $m_1 = (3 - 20) \cdot 10^{-2}$  eV, is similar in all cases.

The upper bounds on  $m_{ee}$  as functions of  $m_1$  have a similar dependence for all the cases. The lower bounds are different and depend on specific values of oscillation parameters.

Thus, for the LMA solutions a lower bound exists in the range of mass hierarchy ( $m_1 < 10^{-3}$  eV) if the solar mixing angle is sufficiently large (see fig. 16 a)). In this case the contribution from  $\nu_2$  dominates and no cancellation is possible even for maximal possible  $m_{ee}^{(3)}$ . In contrast, for a lower  $\sin^2 2\theta_\odot$  the cancellation can be complete so that no lower bound appears (see fig. 16 a)).

In the first transition region all states contribute with comparable portions to  $m_{ee}$ , thus cancellation is possible and no lower bound exists.

In the second transition region as well as in the completely degenerate case the first and the second state give the dominating contributions to  $m_{ee}$  and the increase of  $m_3$  does not influence significantly the total  $m_{ee}$ . The mass  $m_{ee}$  is determined by  $m_1$  and  $\theta_\odot$ . Moreover, a larger  $\sin^2 2\theta_\odot$  implies a larger possible range of  $m_{ee}$  for a given  $m_1$  (fig. 16 a,b)).

Let us consider the SMA MSW solution (fig. 16 d)). In the mass hierarchy region the third state gives the main contribution and no lower bound exists. A lower bound on  $m_{ee}$  appears at  $m_1 > 1.5 \cdot 10^{-3}$  eV and at  $m_1 > 10^{-2}$  eV, where the mass  $m_{ee}$  is given by  $m_1$ .

In the case of the VO solution (fig. 16 c) the upper bound on  $m_{ee}$  is given by  $m_{ee}^{(3)}$  up to  $m_1 \sim 2 \cdot 10^{-4}$  eV. In the range of partial degeneracy the contribution from the first and the second states become important. No lower bound on  $m_{ee}^{(3)}$  can be established from the present data in the whole range of  $m_1$ .

## 7 Scheme with inverse mass hierarchy

Let us consider the partially degenerate spectrum with

$$m_3^2 \approx m_2^2 = \Delta m_{atm}^2, \quad m_1^2 \ll m_2^2, \quad \Delta m_{23}^2 = \Delta m_\odot^2, \quad (65)$$

so that the mass of the second and third neutrino are determined from the atmospheric neutrino data. The  $\nu_e$  flavor is concentrated in the heavy states (inverse mass hierarchy). A small admixture of  $\nu_e$  in the lightest state can exist (fig. 17 ).

The contribution to  $m_{ee}$  from the first state equals

$$m_{ee}^{(1)} = m_1 U_{e1}^2. \quad (66)$$

The inequality  $m_1^2 \ll \Delta m_{atm}^2$  implies  $m_1 < 2 \cdot 10^{-2}$  eV for  $m_1^2/m_2^2 < 0.1$ . Using then the CHOOZ result which restricts (in schemes with inverse hierarchy)  $U_{e1}^2$ :  $U_{e1}^2 < 2.5 \cdot 10^{-2}$ , we get

$$m_{ee}^{(1)} < 5 \cdot 10^{-4} \text{ eV}. \quad (67)$$

The sum of the contributions from the two heavy degenerate states can be written as

$$m_{ee}^{(2)} + m_{ee}^{(3)} \simeq \sqrt{\Delta m_{atm}^2} (\sin^2 \theta_\odot + e^{i\phi_{23}} \cos^2 \theta_\odot), \quad (68)$$

where  $\phi_{23} \equiv \phi_2 - \phi_3$ . For the SMA solution we get from eq. (68)

$$m_{ee} \approx m_{ee}^{(2)} + m_{ee}^{(3)} \approx \sqrt{\Delta m_{atm}^2} = (4 - 8) \cdot 10^{-2} \text{ eV} \quad (69)$$

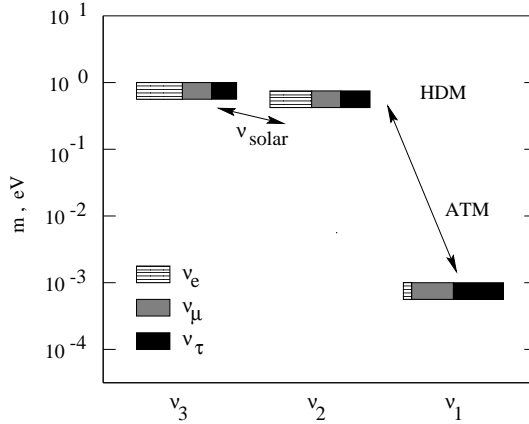


Figure 17: The neutrino mass and mixing pattern in the bi-large mixing scheme with inverse mass hierarchy.

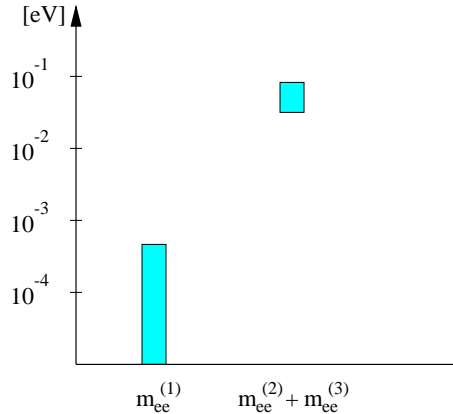


Figure 18: Contributions to  $m_{ee}$  from different mass eigenstates in the scheme with inverse mass hierarchy and SMA solution. The degenerate states give the main contribution, implying a unique prediction for  $m_{ee}$ .

and in the bestfit point of the atmospheric neutrino data:  $m_{ee} \approx 6 \cdot 10^{-2}$  eV. This means, that the predicted value of  $m_{ee}^2$  coincides with  $\Delta m_{atm}^2$  (fig. 18). This coincidence provides a unique possibility to identify the scheme (see also, e.g. [12]).

The relation  $m_{ee}^2 = \Delta m_{atm}^2$  applies also for the case of the LMA solution as long as  $\phi_2 = 0$ <sup>2</sup>.

For the LMA solution the sum of the contributions from the two heavy states lies in the interval

$$m_{ee}^{(2)} + m_{ee}^{(3)} = (\cos 2\theta_\odot - 1) \cdot \sqrt{\Delta m_{atm}^2}. \quad (70)$$

For  $\sin^2 2\theta_\odot < 0.98$  we get  $m_{ee} > 4 \cdot 10^{-3}$  eV which is still much larger than  $m_{ee}^{(1)}$ . The compensation is complete if the mixing is maximal. The value  $m_{ee}^{(2)} + m_{ee}^{(3)} < 2 \cdot 10^{-3}$  eV

<sup>2</sup>Notice that if the mass degeneracy originates from some flavor blind interactions one may indeed expect that masses of  $\nu_2$  and  $\nu_3$  have the same phase.

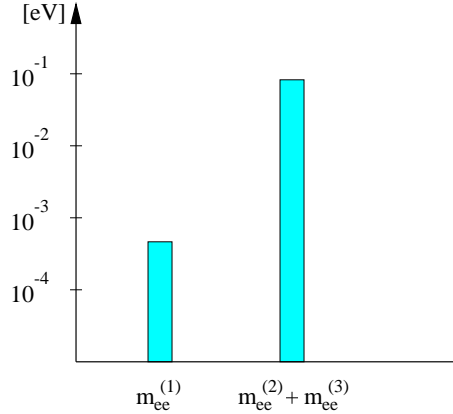


Figure 19: Contributions to  $m_{ee}$  from different mass eigenstates in the schemes with inverse hierarchy and LMA, LOW or VO solutions. Now cancellation between the degenerate states is possible leading to a wide range of values allowed for  $m_{ee}$ .

requires a very small deviation from maximal mixing:  $1 - \sin^2 2\theta_\odot < 2 \cdot 10^{-3}$ . Thus, the lower bound on  $m_{ee}$  can be further strengthened, if the deviation from maximal mixing will be established.

A similar consideration holds for the cases of LOW MSW or vacuum oscillation solutions (69) (see fig. 19).

The contribution of the two heavier eigenstates to the HDM,  $\Omega_\nu = (2m_1)/(91.5 \text{ eV} h^2) \sim 0.01$ , is rather small and below the reach of future projects on measurements of cosmological parameters.

If the  $\nu_e$  admixture in the lightest state is non-zero, so that the  $\nu_e$ -oscillations driven by  $\Delta m^2$  exist, the scheme can be identified by studying matter effects in atmospheric and supernova neutrinos as well as in the long-baseline experiments.

Indeed, in the case of inverse mass hierarchy the  $\nu_e - \bar{\nu}_3'$  level crossing (in matter) occurs in the *antineutrino* channel, so that in supernovae the antineutrinos  $\bar{\nu}_e$  will be strongly converted into a combination of  $\bar{\nu}_\mu$ ,  $\bar{\nu}_\tau$  and vice versa. This leads to a hard  $\bar{\nu}_e$ 's spectrum at the Earth detector which coincides with the original  $\bar{\nu}_\mu$  spectrum [37].

In atmospheric neutrinos the identification of the type of mass hierarchy will be possible if the sensitivity will be enough to detect oscillation effects in e-like events (electron neutrinos and antineutrinos). It will be also important to measure the sign of the electric charge of the lepton, since the matter effects are different in the neutrino and antineutrino channels and this difference depends on the type of mass hierarchy.

These matter effects can be studied in LBL experiments [39, 40] with neutrinos from neutrino factories where beams of neutrinos and antineutrinos are well controlled.

Let us consider the dependence of the predictions for  $m_{ee}$  on  $m_1$ . In the schemes with inverse hierarchy there is only one transition region:  $m_1 \sim \sqrt{\Delta m_{atm}^2}$ , that is  $m_1 \sim m_2 \approx m_3$  or  $m_1 = (1-8) \cdot 10^{-2} \text{ eV}$ . The sum of the contributions from the second and the third states dominates in the whole range of  $m_1$ . It is determined by the “solar” mixing angle

$\theta_\odot$  and  $m_2 \approx m_3$ . The latter changes from  $\sqrt{\Delta m_{atm}^2}$  in the hierarchical region to  $m_1$  in the region of complete degeneracy (see fig. 16 e-h). The mass  $m_{ee}$  is completely predicted in terms of  $m_2$  for the SMA solution (fig. 16 h).

No lower bound on  $m_{ee}$  appears when the (solar) mixing parameter is maximal or close to maximal.

## 8 Four neutrino scenarios

The introduction of new (“sterile”) neutrinos mixed with the usual SU(2) doublet neutrinos opens new possibilities for the construction of the neutrino mass spectrum and for the explanation of the data. It also modifies predictions of  $m_{ee}$ . Here we will consider several scenarios which are motivated both by phenomenology and theory. All scenarios we will discuss contain one or two (degenerate) states in the range relevant for structure formation in the universe and/or for the LSND oscillations.

### 8.1 Scenario with small flavor mixing and mass hierarchy

The scheme (fig. 20) is characterized by a mass hierarchy:

$$m_4 = m_{HDM}, \quad m_3 \approx \sqrt{\Delta m_{ATM}^2}, \quad m_2 \approx \sqrt{\Delta m_\odot^2}, \quad m_1 \ll m_2. \quad (71)$$

The states  $\nu_\mu$  and  $\nu_s$  are strongly mixed in the second and fourth mass eigenstates, so that  $\nu_\mu \leftrightarrow \nu_s$  oscillations solve the atmospheric neutrino problem. All other mixings are small. In particular, the solar neutrino problem is solved by small mixing MSW conversion  $\nu_e \rightarrow \nu_\mu, \nu_s$ .

The main motivation for this scheme is to avoid the introduction of large mixing between flavor states and to keep in this way as much as possible correspondence with the quark sector.

A clear signature of the scheme is the  $\nu_\mu \leftrightarrow \nu_s$  oscillation solution of the atmospheric neutrino problem. The solution can be tested by (i) studies of the neutral current interactions in atmospheric neutrinos, in particular,  $\nu N \rightarrow \nu N \pi^0$  (with  $N = n, p$ ), which gives the main contribution to the sample of the so called  $\pi^0$  events (the rate should be lower in the  $\nu_\mu \rightarrow \nu_s$  case); (ii) studies of the zenith angle distribution of the upward going muons (stopping and through-going); (iii) detection of the  $\tau$  leptons produced by converted  $\nu_\tau$ .

Recent Super-Kamiokande data do not show a deficit of  $\pi^0$  events, and moreover the  $\nu_\mu \rightarrow \nu_\tau$  oscillations give a better fit (of about  $2-3\sigma$ ) of the zenith angle distribution thus favoring the  $\nu_\mu \rightarrow \nu_\tau$  interpretation. However, more data are needed to draw a definite conclusion (see [30]).

The novel element of this scheme (compared with the  $3\nu$  - schemes discussed in the previous sections) is the existence of a heavy state in the HDM range. Its contribution to  $m_{ee}$  equals:

$$m_{ee}^{(4)} = U_{e4}^2 m_4. \quad (72)$$

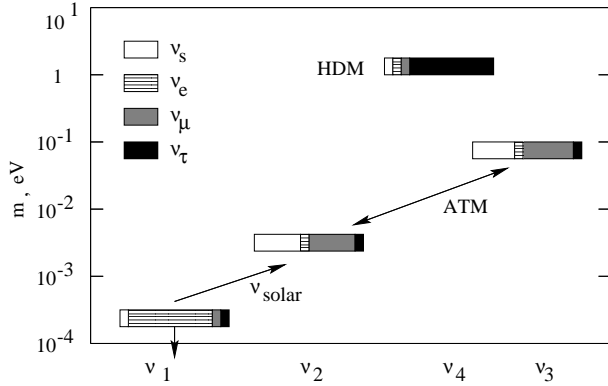


Figure 20: Neutrino masses and mixing in the  $4\nu$  scenario with small flavor mixing and mass hierarchy. Here the white parts of the boxes correspond to admixtures of the sterile state.

The relevant parameters,  $U_{e4}$  and  $m_4$ , can be determined from studies of the short range  $\nu_e \leftrightarrow \nu_e$  oscillations (disappearance) driven by the largest mass splitting  $m_4 \approx \sqrt{\Delta m^2} \approx m_{HDM}$ . For this channel the effective mixing angle equals

$$\sin^2 2\theta_{ee} = 4|U_{e4}|^2(1 - |U_{e4}|^2) \approx 4|U_{e4}|^2, \quad (73)$$

so that

$$m_{ee}^{(4)} \approx \frac{1}{4} \sqrt{\Delta m^2} \sin^2 2\theta_{ee}. \quad (74)$$

The corresponding iso-mass lines in the  $\Delta m^2 - \sin^2 2\theta$  plot together with various oscillation bounds are shown in fig. 21.

In the cosmologically interesting range,  $\sqrt{\Delta m^2} \approx m_{HDM} \simeq (0.5 - 5)$  eV, the mixing is constrained by the BUGEY experiment:  $\sin^2 2\theta_{ee} = (2 - 4) \cdot 10^{-2}$ . Therefore we get the upper bound

$$m_{ee}^{(4)} \simeq (2 - 5) \cdot 10^{-2} \text{ eV}. \quad (75)$$

There is no strict relation between  $m_{ee}$  and the parameters of the  $\nu_e \leftrightarrow \nu_\mu$  oscillations since both relevant mixing elements  $U_{e3}$  and  $U_{\mu 3}$  are small. Indeed, now the effective depth of oscillations is determined by  $\sin^2 2\theta_{e\mu} = 4|U_{e3}|^2|U_{\mu 3}|^2$ , so that

$$m_{ee}^{(4)} = \frac{\sin^2 2\theta_{e\mu} m_{HDM}}{4|U_{\mu 4}|^2}. \quad (76)$$

It is impossible to infer useful information from this unless the  $U_{\mu 4}$  will be determined from other experiments. Taking the bound  $|U_{\mu 4}|^2 < 0.25$  from the  $3\nu$  - analysis of the atmospheric neutrino data, we get from eq. (76) the lower bound

$$m_{ee}^{(4)} > \sin^2 2\theta_{e\mu} m_{HDM}. \quad (77)$$

To get an estimation we assume  $\sin^2 2\theta_{e\mu} \sim 10^{-3}$  which corresponds to upper bounds on the elements  $U_{e4}$  and  $U_{\mu 4}$  from the BUGEY experiment and searches for  $\nu_\mu \leftrightarrow \nu_\tau$

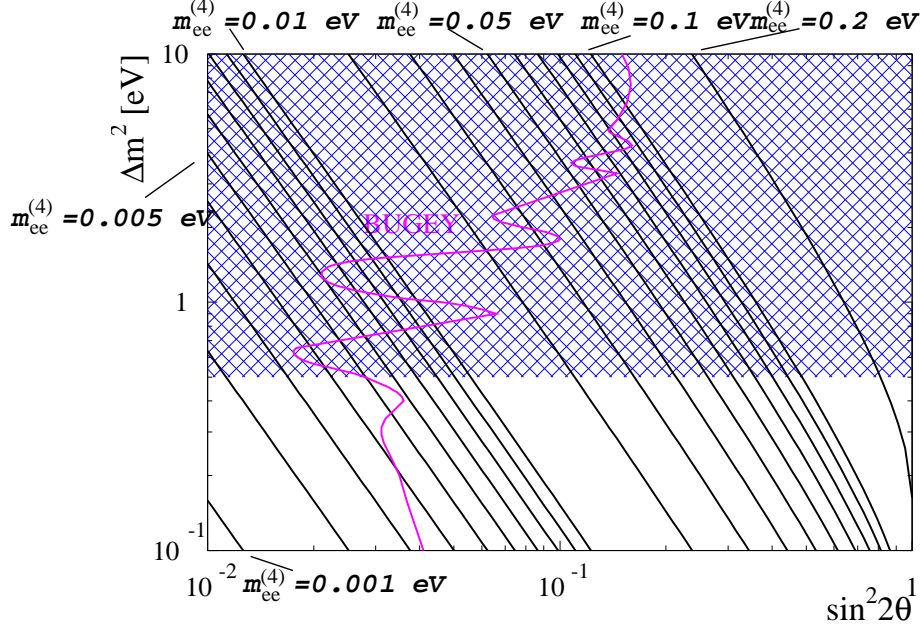


Figure 21: Iso-mass  $|m_{ee}^{(4)}|$  lines in the four-neutrino scenario with small flavor mixing and mass hierarchy. The shadowed area shows the region for neutrino masses of cosmological interest as HDM. Also shown are the regions excluded by the reactor experiment BUGEY (from [49]).

oscillations. (Notice that LSND result can not be completely explained in this scheme.) This leads to

$$m_{ee}^{(4)} \gtrsim 10^{-3} \text{ eV} . \quad (78)$$

The contributions from the three light states are similar to the contributions in the  $3\nu$  single maximal mixing scheme with mass hierarchy (sect. 3.1). In particular, the largest contribution may come from the third mass eigenstate:  $m_{ee}^{(3)} = \sqrt{\Delta m_{atm}^2} U_{e3}^2 < 2 \cdot 10^{-3}$  eV (see eq. (32)). The contributions from the two lightest states can be estimated as  $m_{ee}^{(2)} = (5 \cdot 10^{-7} - 10^{-5})$  eV and  $m_{ee}^{(1)} < 2 \cdot 10^{-3}$  eV.

Thus, the  $0\nu\beta\beta$ -mass (see fig. 22) can be dominated by the contribution of the heaviest state which can reach  $m_{ee} \approx m_{ee}^{(4)} \sim 5 \cdot 10^{-2}$  eV.

The contribution depends strongly on the mixing angle  $\sin^2 2\theta_{e\tau}$ . Short baseline experiments (such as the rejected short baseline neutrino oscillation proposal TOSCA) could in principle test the region of large masses  $m_{HDM} \simeq 10$  eV down to  $\sin^2 2\theta_{e\tau} = 10^{-3}$ , which correspond to an improvement of the upper bound on  $m_{ee}$  by 1 - 2 orders of magnitude. Due to possible cancellations between the contributions no lower bound on  $m_{ee}$  can be obtained from the present data.

Notice that the MINIBOONE experiment will probe the mixing angle  $\sin^2 2\theta_{e\mu}$  down to  $4 \cdot 10^{-4}$  eV and thus will check the LSND result. A confirmation of the LSND result will exclude this scheme.

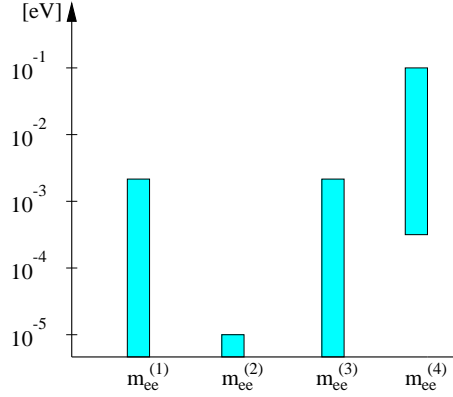


Figure 22: Contributions to  $m_{ee}$  from different mass eigenstates in the  $4\nu$  scheme with small flavor mixing and mass hierarchy.

## 8.2 Scenario with two heavy degenerate neutrinos

The main motivation for this scenario (see fig. 23) is to explain the LSND result along with oscillation solutions of the solar and atmospheric neutrino problems [50, 51]. The masses are determined as

$$m_3 \approx m_4 \approx \sqrt{\Delta m_{LSND}^2}, \quad m_2 \approx \sqrt{\Delta m_{\odot}^2}, \quad m_1 \ll m_2. \quad (79)$$

The neutrinos  $\nu_\mu$  and  $\nu_\tau$  are strongly mixed in the two heavy mass eigenstates  $\nu_2$  and  $\nu_3$ , so that  $\nu_\mu \leftrightarrow \nu_\tau$  oscillations solve the atmospheric neutrino problem. The two other neutrinos,  $\nu_e$  and  $\nu_s$ , are weakly mixed in the two lightest mass states and the resonance  $\nu_e \rightarrow \nu_s$  conversion solves the solar neutrino problem.

The two heavy neutrinos with masses  $m_3 \approx m_4$  can be relevant for cosmology, their contribution to a hot dark matter component equals:

$$m_{HDM} = 2m_3 = 2\sqrt{\Delta m_{LSND}^2}. \quad (80)$$

In this scheme the new element is the existence of two heavy degenerate states. Let us consider in details their contribution to  $m_{ee}$  (the effect of the two lightest states is small). Using relations (79) we can write this contribution as

$$m_{ee}^{(3)} + m_{ee}^{(4)} \approx (|U_{e3}|^2 + |U_{e4}|^2 e^{i\phi_{34}}) \sqrt{\Delta m_{LSND}^2} \quad (81)$$

and  $\phi_{34} \equiv \phi_4 - \phi_3$  is the relative phase of the  $\nu_3$  and  $\nu_4$  masses. Let us express the masses in eq. (81) in terms of oscillation parameters. In short base-line experiments the only oscillation phases which enter are the ones between heavy states and light states. One can neglect the oscillation phase between the two light states which is determined by  $\Delta m_{\odot}^2$  and the phase between the two heavy states which is determined by  $\Delta m_{atm}^2$ . In this case the oscillations are reduced to two neutrino oscillations with a phase determined by  $\Delta m_{LSND}^2$  and the width for the  $\nu_e \leftrightarrow \nu_\mu$  channel:

$$\sin^2 2\theta_{e\mu} = 4|U_{e3}^* U_{\mu 3} + U_{e4}^* U_{\mu 4}|^2. \quad (82)$$

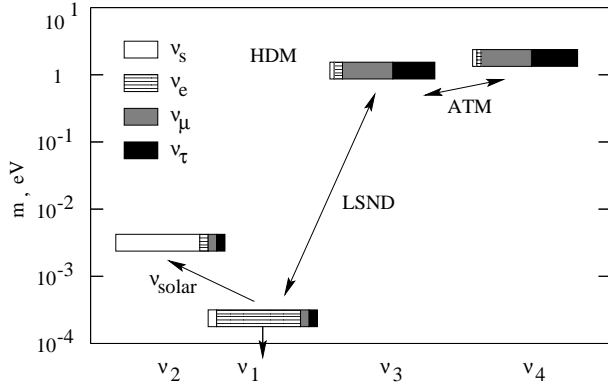


Figure 23: The pattern of the neutrino mass and mixing in the scheme with two degenerate neutrinos and one sterile component.

Let us consider two extreme situations: suppose an admixture of the  $\nu_e$  flavor in one of the heavy states is much larger than in the other one, *e.g.*  $|U_{e3}| \gg |U_{e4}|$ , then  $\sin^2 2\theta_{e\mu} = |U_{e3}|^2 |U_{\mu 3}|^2$ , and therefore  $|U_{e3}|^2 = \sin^2 2\theta_{e\mu} / |U_{\mu 3}|^2$ . In this case we get from eq. (81)  $m_{ee}^{(3)} + m_{ee}^{(4)} \approx |U_{e3}|^2 m_3$ , and consequently,

$$m_{ee}^{(3)} + m_{ee}^{(4)} \approx \frac{\sin^2 2\theta_{e\mu}}{|U_{\mu 3}|^2} \sqrt{\Delta m_{LSND}^2}. \quad (83)$$

Since  $|U_{\mu 3}|^2 \sim 0.5$  is determined by atmospheric neutrino oscillations, taking  $\sin^2 2\theta_{e\mu} = 2 \cdot 10^{-3}$  and  $\sqrt{\Delta m_{LSND}^2} = 1$  eV we find  $m_{ee}^{(3)} + m_{ee}^{(4)} \approx 10^{-3}$  eV.

Let us now take  $U_{e3}^* U_{\mu 3} \approx U_{e4}^* U_{\mu 4}$ , then  $\sin^2 2\theta_{e\mu} = 16 |U_{e3}^* U_{\mu 3}|$  and  $m_{ee}^{(3)} + m_{ee}^{(4)} \approx \sin^2 2\theta_{e\mu} \sqrt{\Delta m_{LSND}^2} / 2$ , provided that the two contributions are in phase. This result is two times smaller than the result in the previous case.

For the  $\nu_e \leftrightarrow \nu_e$  channel we find the depth of oscillations

$$\sin^2 2\theta_{ee} = 4U_+ (1 - U_+) \approx 4U_+, \quad (84)$$

where  $U_+ \equiv |U_{e3}|^2 + |U_{e4}|^2$ . At the same time  $m_{ee} \leq U_+ \sqrt{\Delta m_{LSND}^2} / 2$ , so that

$$m_{ee}^{(3)} + m_{ee}^{(4)} \approx \frac{1}{4} \sin^2 2\theta_{ee} \sqrt{\Delta m_{LSND}^2}. \quad (85)$$

Using the BUGEY bound on  $\sin^2 2\theta_{ee}$  we get  $m_{ee}^{(3)} + m_{ee}^{(4)} \lesssim 10^{-2}$  eV.

Since cancellations may show up, no lower bound can be obtained.

The same combination of neutrino mixing matrix elements (84) determines the  $\nu_e$  mode of oscillations in atmospheric neutrinos. It will lead to an overall suppression of the number of the  $e$ -like events.

The contributions from the light states are similar to those in the  $3\nu$  case (see sect. 3.1):  $m_{ee}^{(2)} = (5 \cdot 10^{-7} - 10^{-5})$  eV and  $m_{ee}^{(1)} \ll 2 \cdot 10^{-3}$  eV.

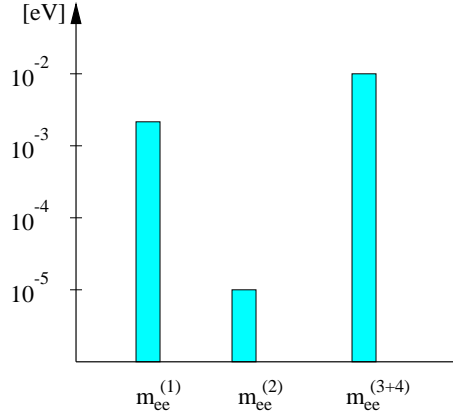


Figure 24: Contributions to  $m_{ee}$  from different mass eigenstates for the  $4\nu$  scheme with two degenerate pairs of neutrinos and normal mass hierarchy.

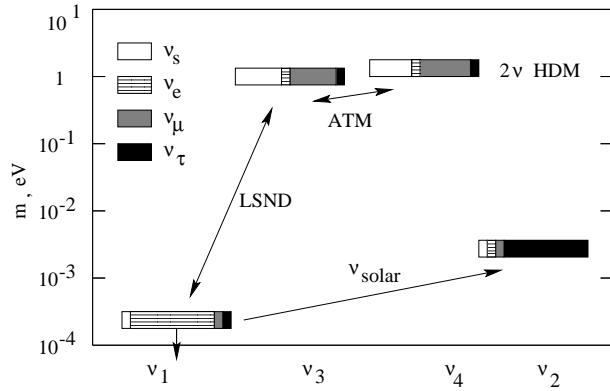


Figure 25: The neutrino masses and mixing in the “Grand Unification” scenario.

Summing up all the contributions we get that the  $0\nu\beta\beta$ -mass can be at most (*few*)  $\times 10^{-2}$  eV being dominated by the contribution of the heavy states at the upper bound (fig. 24). A coincidence of a  $0\nu\beta\beta$  decay signal in this range with a confirmation of the LSND oscillations by MINIBOONE can be considered as a hint for this scheme. At the same time, since cancellation between different contributions can show up, no lower bound on  $m_{ee}$  exists. Thus, a non-observation of  $0\nu\beta\beta$  decay of the order of magnitude (*few*)  $\cdot 10^{-2}$  eV does not rule out the scheme.

A similar situation appears in the “Grand Unification” scenario [52, 53] which is characterized by strong mixing of  $\nu_\mu$  and  $\nu_s$  in the two heavy states and mixing of  $\nu_e$  and  $\nu_\tau$  in the two light states (fig. 25). Here the atmospheric neutrino problem is solved by  $\nu_\mu \leftrightarrow \nu_s$  oscillations whereas the solar neutrino data are explained by  $\nu_e - \nu_\tau$  conversion.

### 8.3 Scenario with inverse mass hierarchy

The mass hierarchy in the two schemes with two pairs of states with small splitting can be inverse. In the first case,  $\nu_e$  and  $\nu_s$  flavors are concentrated in the two heavy states  $\nu_3$  and  $\nu_4$ , whereas  $\nu_\mu$  and  $\nu_\tau$  are in the two light states. The dominating contribution comes from the third state which almost coincides with  $\nu_e$ :

$$m_{ee} \approx m_{ee}^{(3)} \approx \sqrt{\Delta m_{LSND}^2} \approx 0.4 - 1 \text{ eV}. \quad (86)$$

Thus in the context of this scheme the double beta decay searches check immediately the LSND result, and in fact, already existing data disfavor the scheme.

Another possibility of the inverse hierarchy is that the  $\nu_e$  and  $\nu_\tau$  flavors are concentrated in the heavy states, whereas  $\nu_\mu$  and  $\nu_s$  are in the pair of light mass states whose splitting leads to the atmospheric neutrino oscillations. The situation is similar to that for the  $3\nu$  scheme with inverse hierarchy (see sect. 7) with the only difference that  $\Delta m_{atm}^2$  should be substituted by  $\Delta m_{LSND}^2$ :

$$m_{ee}^{(3)} + m_{ee}^{(4)} \simeq \sqrt{\Delta m_{LSND}^2} (\sin^2 \theta_\odot + e^{i\phi_{23}} \cos^2 \theta_\odot). \quad (87)$$

The third and the fourth mass eigenstates give the dominating contributions. Thus the expected interval for the total effective mass is

$$m_{ee} \approx \sqrt{\Delta m_{LSND}^2} (\cos 2\theta_\odot - 1). \quad (88)$$

This interval can be probed already by existing experiments, although for large mixing angle solutions of the solar neutrino problem (LMA, LOW, VO) strong cancellation can occur.

## 9 Discussion and Conclusions

In fig. 26 we summarize the predictions for  $m_{ee}$  in various schemes considered in this paper. We also show the present upper bound of  $0\nu\beta\beta$  decay experiments [44] and regions of sensitivity which can be reached in future double beta decay experiments. Future double beta decay projects such as GENIUS [54, 13, 55], CUORE [56], MOON [57] will lead to a significant improvement of the sensitivity. The most ambitious and at the same time most realistic project, GENIUS, will test  $m_{ee}$  down to  $2 \cdot 10^{-2}$  eV in the one ton version with one year of measurement time and down to  $2 \cdot 10^{-3}$  eV in the 10 ton version with 10 years of measurement time.

According to figure 26 there are two key scales of  $m_{ee}$ , which will allow one to discriminate among various schemes:  $m_{ee} \sim 0.1$  eV and  $m_{ee} = 0.005$  eV.

1). If future searches will show that  $m_{ee} > 0.1$  eV, then the schemes which will survive are those with neutrino mass degeneracy or  $4\nu$  schemes with inverse mass hierarchy. All other schemes will be excluded.

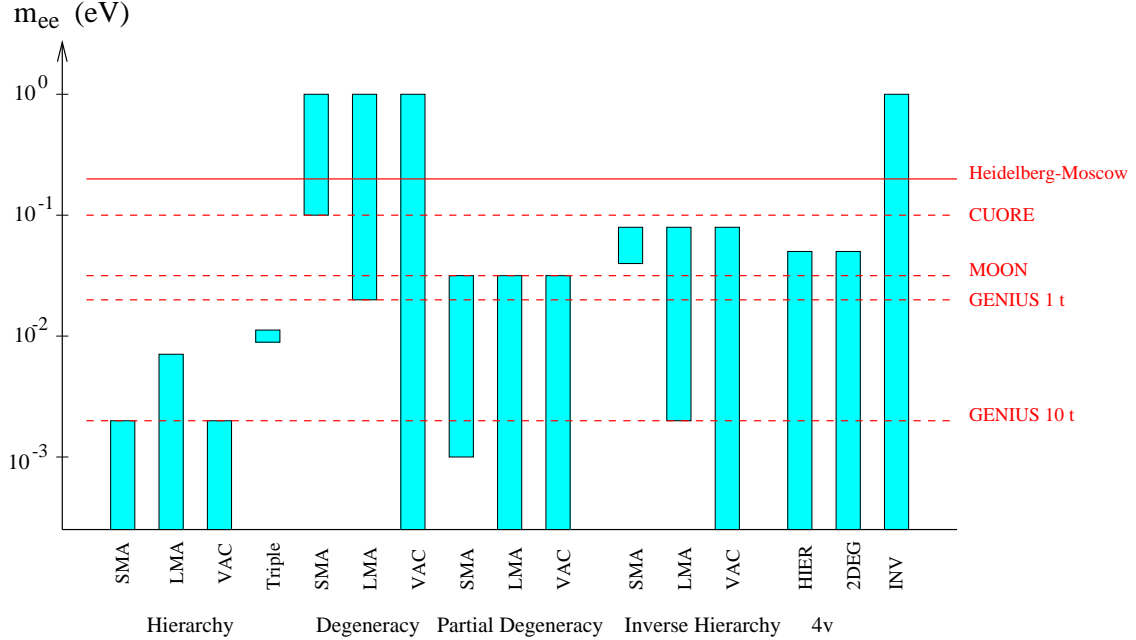


Figure 26: Summary of expected values for  $m_{ee}$  in the different schemes discussed in this paper. The expectations are compared with the recent neutrino mass limits obtained from the Heidelberg–Moscow [44] experiment as well as the expected sensitivities for the CUORE [56], MOON [57] proposals and the 1 ton and 10 ton proposal of GENIUS [13].

2). For masses in the interval  $m_{ee} = 0.005 - 0.1$  eV, possible schemes include:  $3\nu$  schemes with partial degeneracy, triple maximal scheme,  $3\nu$  schemes with inverse mass hierarchy and  $4\nu$  scheme with one heavy ( $O(1$  eV)) neutrino.

3). If  $m_{ee} < 0.005$  eV, the schemes which survive are  $3\nu$  schemes with mass hierarchy, schemes with partial degeneracy, and the  $4\nu$  schemes with normal hierarchy. The schemes with degenerate spectrum and inverse mass hierarchy will be excluded, unless large mixing allows for strong cancellations. For  $m_{ee} < 0.001$  eV this applies also for schemes with a partial degenerate spectrum.

Future oscillation experiments will significantly reduce the uncertainty in predictions for  $m_{ee}$  and therefore modify implications of  $0\nu\beta\beta$  decay searches. Before a new generation of  $0\nu\beta\beta$  decay experiments will start to operate we can expect that

- The solution of the solar neutrino problem will be identified. Moreover,  $\Delta m_{\odot}^2$  and  $\sin^2 2\theta_{\odot}$  will be determined with better accuracy. In particular, in the case of the solutions with large mixing (LMA, LOW, VO) the deviation of  $1 - \sin^2 2\theta_{\odot}$  from zero can be established.
- The dominant channel of the atmospheric neutrino oscillation ( $\nu_{\mu} - \nu_{\tau}$  or  $\nu_{\mu} - \nu_s$ ) will be identified. The mass  $\Delta m_{atm}^2$  will be measured with better precision.

- A stronger bound on the element  $U_{e3}$  will be obtained or it will be measured if oscillations of electron neutrinos to tau neutrinos driven by  $\Delta m_{atm}^2$  will be discovered in the atmospheric neutrino or LBL experiments.
- The LSND result will be checked by MINIBOONE.

In the following we summarize possible consequences of these oscillation results.

1). Let us first comment on how the identification of the solution of the solar neutrino problem will modify implications of the  $0\nu\beta\beta$  decay searches.

- If the SMA solution of the solar neutrino problem turns out to be realized in nature, a value of  $m_{ee} > 0.2$  eV will imply a completely degenerate neutrino mass spectrum or schemes with inverse mass hierarchy. The measured value of  $m_{ee}$  will coincide with  $m_1$  and will fix the absolute mass scale in the neutrino sector. A confirmation of this conclusion can be obtained from the CMB experiments MAP and Planck, if the degenerate neutrino mass is larger than  $\simeq 0.4$  eV. However this value is already disfavored by the recent limits obtained from the Heidelberg-Moscow experiment.

For lower values,  $m_{ee} = 2 \cdot 10^{-3} - 10^{-2}$  eV, a scheme with partially degenerate spectrum will be favored. Again, we have  $m_{ee} = m_1$  and the mass scale can be fixed.

For even lower mass values:  $m_{ee} < 2 \cdot 10^{-3}$  eV, or, after MINOS improved the bound on  $m_{ee}^{(3)}$ ,  $m_{ee} \lesssim 4 \cdot 10^{-4}$  eV, with the contribution  $m_{ee}^{(3)}$  a new parameters enters, which for larger  $m_{ee}$  could be neglected. Thus it will be impossible to quantify the contribution of each single state to  $m_{ee}$ , unless  $m_{ee}^{(3)}$  will be fixed in atmospheric or LBL oscillations.

- If the LMA solution of the solar neutrino deficit turns out to be realized in nature, a value  $m_{ee} > 2 \cdot 10^{-2}$  eV will testify for a scenario with degenerate mass spectrum. A confirmation of this result will be obtained from the CMB experiments MAP and Planck, if the degenerate neutrino mass is larger than  $\simeq 0.4$  eV. Using the mixing angle determined in solar neutrino experiments the range for the absolute mass scale can be determined from  $m_{ee}$  according to fig. 14. A value of  $m_{ee} < 2 \cdot 10^{-2}$  eV will favor schemes with partial degeneracy or hierarchical spectrum. As soon as  $m_{ee} < 2 \cdot 10^{-3}$  eV  $m_{ee}^{(3)}$  becomes important and enters as a new parameter and it will be difficult to reconstruct the type of hierarchy.
- If the LOW or VO solution is the solution of the solar neutrino problem, the situation is similar to the MSW LMA case. The only difference is, that an observed  $0\nu\beta\beta$ -mass  $m_{ee} > 2 \cdot 10^{-3}$  eV will imply a partially or completely degenerate scheme. Below this value the type of hierarchy can not be identified until bounds on  $m_{ee}^{(3)}$  will be improved.

For schemes with inverse mass hierarchy the situation can be more definite:

- If the MSW SMA solution turns out to be true, a value of  $m_{ee} = \sqrt{\Delta m_{atm}^2} = (5 - 8) \cdot 10^{-2}$  eV is expected. This value coincides with  $m_1 \simeq m_2$  and therefore will give the absolute mass scale. For larger masses:  $m_{ee} > 8 \cdot 10^{-2}$  eV the transition to a completely degenerate spectrum occurs.
- If the MSW LMA, MSW LOW or vacuum oscillation solution is realized, a value of  $m_{ee} = (0.02 - 8) \cdot 10^{-2}$  eV will testify for inverse mass hierarchy. The interval of expected values of  $m_{ee}$  can be narrower once the deviation of  $1 - \sin^2 2\theta$  from zero will be measured in solar neutrino experiments.

For larger values of masses:  $m_{ee} > 8 \cdot 10^{-2}$  eV the scheme approaches the degenerate case.

2). The discovery of a sterile neutrino will have significant impact on the implications of the double beta decay searches.

The existence of a sterile neutrino can be established by a confirmation of the LSND result in MINIBOONE, or by a proof of the  $\nu_e \rightarrow \nu_s$  oscillations solution of the solar neutrino problem by SNO, or by studies of the atmospheric neutrinos.

For 4  $\nu$  scenarios the interpretation of the  $0\nu\beta\beta$  decay results is rather ambiguous. A value of  $m_{ee} > (few) \times 10^{-2}$  eV will favor the intermediate mass scale scenario, while a value of  $m_{ee} < 10^{-3}$  eV will favor a scenario with two degenerate pairs of neutrinos and normal mass hierarchy. A value of  $m_{ee} > 10^{-1}$  eV will clearly favor an inverse mass hierarchy scheme. In all cases it will be difficult to disentangle the single contributions and to identify a specific spectrum. Important input in this case may come from the CMB experiments MAP and Planck by fixing the mass of the heaviest state.

3).  $U_{e3}$ : further searches for  $\nu_e$  oscillations in atmospheric neutrinos, LBL and reactor experiments will allow one to measure or further restrict this mixing element. This, in turn, will be important for sharpening the predictions for  $m_{ee}$  especially in the schemes with strong mass hierarchy.

4). Matter effects and hierarchy: Studies of matter effects on neutrino oscillations will allow to establish the type of mass hierarchy, which in turn is of great importance for predictions of  $m_{ee}$ .

We can conclude from this summary, that in  $3\nu$  scenarios any measurement of  $m_{ee} > 2 \cdot 10^{-3}$  eV in  $0\nu\beta\beta$  decay (corresponding to the final sensitivity of the 10 ton version of GENIUS) will provide informations about the character of hierarchy of the neutrino mass spectrum and in some cases also to fix the absolute mass scale of neutrinos. For values of  $m_{ee} < 2 \cdot 10^{-3}$  eV no reconstruction of the spectrum is possible until the contribution  $m_{ee}^{(3)}$  will be fixed or bounded more stringent in atmospheric or LBL neutrino oscillations. For four-neutrino scenarios it will be not that easy to fix the mass scale of the neutrino sector. Crucial informations can be obtained from tests of the LSND signal and cosmology.

As has been mentioned before, a non-zero  $0\nu\beta\beta$  decay rate always implies a non-vanishing neutrino Majorana mass [4]. Let us comment finally on possible ambiguities in the interpretation of a positive signal in neutrinoless double beta decay in terms of  $m_{ee}$ , in view of the existence of different alternative mechanisms, which could induce neutrinoless double beta decay, such as R-parity violating SUSY, right-handed currents, or leptoquarks. While no absolute unique method to identify the mechanism being responsible for neutrinoless double beta decay exists, the following remarks can be done:

- 1). Many of the possible alternative contributions require new particles, *e.g.* SUSY partners, leptoquarks, right-handed W bosons or neutrinos having masses in or below the TeV range, which to date not have been observed. Thus one expects to observe effects of new particles at future high energy colliders as the LHC or the NLC, giving independent informations on possible contributions to  $0\nu\beta\beta$  decay (keeping in mind an uncertainty in nuclear matrix elements of about a factor of  $\mathcal{O}(2)$ ). Notice that the same new interactions mentioned here may induce effects in neutrino oscillations and imply ambiguities in the interpretation of the data also there (see *e.g.* [58, 59]).
- 2). Using different source isotopes in different experiments and figuring out the values of  $0\nu\beta\beta$  decay nuclear matrix elements for different contributions may help to identify the dominant one. Also a future experiment being sensitive to angular correlations of outgoing electrons could be useful in the discrimination of different contributions. Observing a positive signal in  $0\nu\beta\beta$  decay should encourage new experimental efforts to confirm the results.
- 3). Last but not least and as discussed in this paper, a non-zero  $0\nu\beta\beta$  decay signal can be related to some experimental results (both positive and negative) in neutrino oscillations and cosmology. A coincident and non-contradictory identification of a single neutrino mass scheme from the complementary results in such different experiments thus should be respected as a strong hint for this scheme.

In conclusion, after Super-Kamiokande has established large mixing in atmospheric neutrinos, the simplest neutrino spectrum with strong mass hierarchy and small flavor mixing (which typically predicts an undetectable  $m_{ee}$ ) is excluded. Now the neutrino mass spectrum can exhibit any surprise: it can have a normal or inverse mass hierarchy, be partially or completely degenerate. More than three mass eigenstates can be involved in the mixing. In view of this more complicated situation a detection of a positive signal in future double beta decay searches seems to be rather plausible. We have shown that for a given oscillation pattern any value of  $m_{ee}$  is possible, which is still not excluded by the experimental bounds on the neutrinoless double beta decay half life limit. (A lower bound on  $m_{ee}$  appears in the case of inverse mass hierarchy.) This means that even after all oscillations parameters will be measured no unique prediction of  $m_{ee}$  can be derived. On the other hand this means that double beta decay searches provides informations being independent on informations obtained from oscillation experiments. Combining the results of double beta decay and oscillation searches offers a unique possibility to shed some light on the absolute scale of the neutrino mass, the type of hierarchy and the level of degeneracy of the spectrum. If we want eventually to reconstruct the neutrino mass and flavor spectrum, further searches for neutrinoless double beta decay with increased

sensitivity seem to be unavoidable.

**Note added:** When this paper has been prepared for submission the papers of ref. [60] appeared which discuss similar topics.

## References

- [1] M. Doi, T. Kotani, E. Takasugi, Progr. Theor. Phys. Suppl. 83 (1985) 1;
- [2] T. Tomoda, Rep. Progr. Phys. 54 (1991) 53
- [3] H.V. Klapdor-Kleingrothaus, H. Päs, hep-ph/0002109, talk given at COSMO99, Trieste/Italy; H.V. Klapdor-Kleingrothaus, hep-ex/9901021, Proc. Int. Conf. on Lepton- and Baryon Number Non-Conservation, Trento, Italy, April 20-25 1998, IOP Bristol (1999) ed. H.V. Klapdor-Kleingrothaus and I. Krivosheina, p.251
- [4] J. Schechter, J.W.F. Valle, Phys. Rev. D 25 (1982) 2951
- [5] D. London, hep-ph/9907419, talk given at Beyond the Desert 99, Castle Ringberg, Tegernsee, Germany, June 1999, IOP Bristol 2000, ed. H.V. Klapdor-Kleingrothaus and I. Krivosheina
- [6] V. Lobashev et al. Phys. Lett. B. 460 (1999) 227; Ch. Weinheimer et al., Phys. Lett. B. 460 (1999) 219
- [7] A. A. Klimenko, A. A. Pomansky, A. A. Smolnikov, Proceedings of the Moriond-1985 Workshop on Perspectives in Electroweak Interactions. v. 2 (1985) 303.
- [8] S.T. Petcov, A.Y. Smirnov, Phys. Lett. B. 322 (1994) 109
- [9] S. Bilenky, A. Bottino, C. Giunti, C. Kim, Phys. Rev. D54 (1996) 1881-1890
- [10] S.M. Bilenki, C. Giunti, C.W. Kim, M. Monteno, Phys. Rev. D57 (1998) 6981-6988; hep-ph/9904328
- [11] C. Giunti, Phys. Rev. D 61 (2000) 036002 (hep-ph/9906275); S. Bilenky, C. Giunti, W. Grimus, hep-ph/9809368 Neutrino '98, Nucl. Phys. B 77 (Proc. Suppl.) (1999) ed. Y. Suzuki and Y. Totsuka; S. Bilenky, C. Giunti, hep-ph/9904328 Proc. 'WIN99', Cape Town, south Africa, 24-30 January (1999)
- [12] S.M. Bilenky, C. Giunti, W. Grimus, B. Kayser, S.T. Petcov, hep-ph/9907234, Phys.Lett. B465 (1999) 193-202
- [13] J. Hellmig, H.V. Klapdor-Kleingrothaus, Z. Phys. A 359 (1997) 351; H.V. Klapdor-Kleingrothaus, M. Hirsch, Z. Phys. A 359 (1997) 361; H.V. Klapdor-Kleingrothaus, J. Hellmig, M. Hirsch, J. Phys. G 24 (1998) 483;
- [14] S. Bilenky, C. Giunti, C. Kim, S. Petcov, Phys. Rev. D54 (1996) 4432-4444

- [15] R. Adhikari, G. Rajasekaran, hep-ph/9812361, Phys. Rev. D 61 (2000) 031301
- [16] H. Minakata, O. Yasuda, Phys. Rev. D 56 (1997) 1692-1697
- [17] H. Minakata, O. Yasuda, Nucl. Phys. B 523 (1998) 597-610
- [18] F. Vissani, hep-ph/9708483
- [19] F. Vissani, hep-ph/9904349, Proc. of the “6th Tropical Seminar on Neutrino and Astroparticle Physics”, May 17-21 1999, San Miniato, Italy
- [20] V. Barger, K. Whisnant, Phys. Lett. B 456 (1999) 194-200
- [21] J. Ellis, S. Lola, hep-ph/9904279 Phys. Lett. B 458 (1999) 310-321
- [22] G.C. Branco, M.N. Rebelo, J.I. Silva-Marcos, Phys. Rev. Lett. 82 (1999) 683-686
- [23] H. Georgi, S. L. Glashow, hep-ph/9808293
- [24] T. Fukuyama, K. Matsuda, H. Nishiura hep-ph/9708397
- [25] T. Fukuyama, K. Matsuda, H. Nishiura, hep-ph/9708397; Mod. Phys. Lett. A13 (1998) 2279
- [26] T. Fukuyama, K. Matsuda, H. Nishiura; Phys. Rev. D57 (1998) 5844
- [27] F. Vissani, JHEP 9906 (1999) 022, hep-ph/9906525
- [28] M. Czakon, J. Gluza, M. Zralek, hep-ph/9906381 Phys. Lett. B 465 (1999) 211-218
- [29] T. Kajita, talk given at Beyond the Desert 99, Castle Ringberg, Tegernsee, Germany, June 1999, IOP Bristol 2000, ed. H.V. Klapdor-Kleingrothaus and I. Krivosheina
- [30] N. Fornengo, M.C. Gonzalez-Garcia, J.W.F. Valle, hep-ph/0002147,
- [31] J. N. Bahcall, P. I. Krastev, A. Yu. Smirnov, to be published
- [32] M.C. Gonzalez-Garcia, P.C. de Holanda, C. Pena-Garay, J.W.F. Valle, hep-ph/9906469
- [33] C. Athanassopoulos et al., Phys. Rev. Lett. 81 (1998) 1774-1777 K. Eitel, hep-ex/9909036;
- [34] T.E. Jannakos, hep-ex/9908043
- [35] A.O. Bazarko, hep-ex/9906003
- [36] J. Lesgourgues, S. Pastor, S. Prunet, hep-ph/9912363
- [37] A.S. Dighe, A.Yu. Smirnov, hep-ph/9907423

- [38] M. Apollonio et al. (CHOOZ collab.), hep-ex/9907037, Phys. Lett. B 466 (1999) 415-430
- [39] K. Zuber, hep-ex/9810022
- [40] MINOS detectors technical design report, version 1.0, October 1998, [http://www.hep.anl.gov/ndk/hypertext/minos\\_tdr.html](http://www.hep.anl.gov/ndk/hypertext/minos_tdr.html); we thank Kai Zuber for bringing this reference to our attention
- [41] E.Kh. Akhmedov, A. Dighe, P. Lipari, A.Yu. Smirnov, Nucl. Phys. B 542 (1999) 3
- [42] J. N. Bahcall, P. I. Krastev, A. Yu. Smirnov, Phys. Rev. D 60 (1999) 093001
- [43] P.F. Harrison, D.H. Perkins, W.G. Scott, Phys. Lett. B 196 (1997) 186
- [44] Heidelberg–Moscow Collab., Phys. Rev. Lett 83 (1999) 41
- [45] E. Gawiser, J. Silk, Science 280 (1998) 1405-1411
- [46] J.R. Primack, M.A.K. Gross, astro-ph/9810204, Proc. of the Xth Recontres de Blois “The birth of galaxies”, June 28 - July 4 1998
- [47] D.J. Eisenstein, W. Hu, M. Tegmark astro-ph/9807130, Submitted to ApJ.
- [48] J.N. Bahcall, P.I. Krastev, A.Yu. Smirnov, Phys. Rev. D 58 (1998) 096016
- [49] L. di Lella, hep-ex/9912010
- [50] J.T. Peltoniemi, J.W.F. Valle, Nucl. Phys. B 406 (1993) 409
- [51] D.O. Caldwell, R.N. Mohapatra, Phys. Rev. D 48(1993) 3259
- [52] J.T. Peltoniemi, D. Tommasini, J.W.F. Valle, Phys.Lett.B298:383-390,1993
- [53] A.S. Joshipura, A.Yu. Smirnov, Phys.Lett.B439:103-111,1998
- [54] H.V. Klapdor–Kleingrothaus, in *Beyond the Desert '97 – Accelerator and Non-Accelerator Approaches* (Eds. H.V. Klapdor–Kleingrothaus, H. Päs), Proc. Int. Workshop on Particle Physics beyond the Standard Model, Castle Ringberg, June 8-14, 1997, IOP Publ., Bristol, Philadelphia, p. 485 and Int. J. Mod. Phys. A 13 (1998) 3953
- [55] H. V. Klapdor-Kleingrothaus, L. Baudis, G. Heusser, B. Majorovits, H. Päs, hep-ph/9910205
- [56] E. Fiorini et al., Phys. Rep 307 (1998) 309
- [57] H. Eijiri et al., nucl-ex/9911008
- [58] S. Bergmann, Nucl.Phys. B515 (1998) 363-383

- [59] N. Fornengo, M. C. Gonzalez-Garcia, J. W. F. Valle, hep-ph/9906539
- [60] K. Matsuda, N. Takeda, T. Fukuyama, H. Nishiura, hep-ph/0003055; W. Rodejohann, hep-ph/0003149 M. Czakon, J. Gluza, M. Zralek, hep-ph/0003161.